Coordination Chemistry Reviews, 93 (1989) 87–153
Elsevier Science Publishers B.V., Amsterdam – Printed in The Netherlands

PICOSECOND SPECTROSCOPY OF TRANSITION METAL COMPLEXES

NICK SERPONE and MARY A. JAMIESON

Department of Chemistry, Concordia University, 1455 deMaisonneuve Blvd., West Montreal, Qué. H3G 1M8 (Canada)

(Received 24 March 1988)

CONTENTS

0010-8545/89/$23.45

A. INTRODUCTION

The degradation of energy and materials in a molecular system is one of the basic questions in chemistry. To describe these molecular phenomena, it is necessary to investigate the time-dependent redistribution of energy amongst the various degrees of freedom within a molecule upon excitation to an excited state, and to study the energy exchange and interactions of the excited molecule with its surrounding molecular environment(s). It is the competition between the various pathways of energy degradation (internal conversion, vibrational relaxation, intersystem crossing, intermolecular energy transfer or chemical reaction) and structural change which determines whether light emission or non-radiative physical and chemical processes are predominant.

Until the mid to late 1970s, the photochemist was only able to explore light-induced chemical reactions using standard spectrofluorimetric techniques, conventional flash photolyses (microsecond (μs) time resolution, 10^{-6} s) and nanosecond (1 ns = 10^{-9} s) laser instrumentation. These techniques, however, are only capable of determining overall rates. The lack of direct experimental probes has hindered access to direct knowledge of the electronic states involved, the rates of intersystem crossing, internal conversion, energy transfer and chemical reaction. The advent of picosecond (1 ps = 10^{-12} s) laser instrumentation and techniques has allowed detailed experimental studies by means of transient absorption and transient emission spectroscopy on a time scale (10^{-9}–10^{-12} s) appropriate for the observation of many fundamental chemical and relaxation processes.

In essence, this article will focus on and illustrate the powerful functionality of picosecond emission and transient absorption techniques using modelocked high power lasers and fast detection methods to unravel the primary events that occur upon photoexcitation of coordination complexes. A determination of the emission spectrum identifies the emitting electronic state(s) and affords an estimate of its lifetime. The combination of time-resolved luminescence data and time-resolved absorption spectra of the ground state (ground state bleaching (GSB)) and spectra of all transient excited states (excited state absorption (ESA)) and species may afford a direct measurement of the rates of formation and decay.

The technique generally employed in picosecond transient absorption spectroscopy is the excite-and-probe method. The sample, generally contained in a 2 mm cell of good optical quality (quartz), is excited by the laser pulse and the events are probed by a probe pulse of white light (about 400–750 nm or a pulse of fixed frequency) having the same temporal characteristics as the excitation pulse. It is also common to excite only a small segment of the sample (excitation pulse beam diameter, about 1–1.5

mm) followed by the probe pulse of smaller dimensions (less than 1–1.5 mm). There are several different geometrical arrangements for the picosecond laser double-beam instrumentation, and a variety of detection methods (Vidicons, photomultiplier tubes, silicon photodiodes). The description of these is beyond the scope of this article; the interested reader may consult the various references noted herein for a particular arrangement.

B. SPECTROSCOPY OF METAL CARBONYL COMPOUNDS

The availability of picosecond and subpicosecond techniques has made possible time-resolved studies of reaction dynamics on the same time scale as solvent motion. These studies have shown that the role of the solvent cannot be described completely in terms of bulk properties; rather, the solvating medium can and must be described on a molecular level.

An interesting candidate for such studies is the $Cr(CO)_6$ complex inasmuch as (i) it undergoes photodissociation with a high quantum yield ($\phi = 0.7$) [1,2], (ii) the absorption spectral maximum of the primary intermediate, $Cr(CO)_5S$, is very sensitive to the solvent ligand S, (iii) matrix isolation studies and theoretical calculations reveal that the photogenerated $Cr(CO)_5$ fragment retains a C_{4v} geometry [3–6], and (iv) the $Cr(CO)_5S$ photofragment is stable on the nanosecond time scale, thereby eliminating possible interference by thermal reactions.

The primary decay of electronically excited $Cr(CO)_6$ is the photodissociation of CO to form the $Cr(CO)_5$ intermediate (eqn. (1)), as determined from matrix [3,4] and solution [7–9] photolyses:

$$Cr(CO)_6 \xrightarrow{h\nu} Cr(CO)_5 + CO \tag{1}$$

Transient absorption spectra 25 ps after photolysis of $Cr(CO)_6$ in cyclohexane and tetrahydrofuran (THF) show that both the absorption maxima and the spectral line shape are dependent on the solvent medium [10]. In cyclohexane–THF mixtures, the transient absorption spectra show superposition of the transient absorption bands observed in the neat solvents. Only $(THF)Cr(CO)_5$ is observed immediately following photolysis of $Cr(CO)_6$ in THF at [THF] > 5.0 M [10]. These observations indicate the formation of a solvent coordinated $Cr(CO)_5$ complex (eqn. (2)) corresponding to the transient absorption spectra taken 25 ps after photolysis:

$$Cr(CO)_6 \xrightarrow[\text{cyclohexane–THF}]{h\nu} Cr(CO)_5S \tag{2}$$

(S = cyclohexane, THF)

There is no evidence for uncoordinated $Cr(CO)_5$ in the solution phase

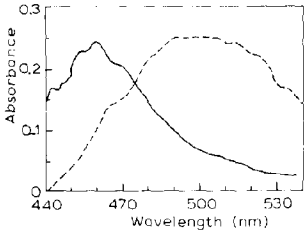

Fig. 1. Transient absorption spectrum of $Cr(CO)_5$(cyclohexane) (----) and $Cr(CO)_5$(methanol) (———) taken 50 ps after photolysis of $Cr(CO)_6$ in cyclohexane and methanol respectively (from ref. 11).

photolysis of $Cr(CO)_6$. The non-statistical partition between (THF)$Cr(CO)_5$ and (cyclohexane)$Cr(CO)_5$ observed in various cyclohexane–THF solvent mixtures arises [10] from differences in frequency factors resulting from dipole interactions created during CO photoelimination. The rate of exchange of cyclohexane from (cyclohexane)$Cr(CO)_5$ with THF to form (THF)$Cr(CO)_5$ is bimolecular and entropically controlled. Temperature-dependence studies of $Cr(CO)_6$ in a 1.0 M THF–cyclohexane mixture yield an enthalpy and entropy of activation of 1 ± 1 kcal mol^{-1} and 20 ± 4 e.u. respectively. The $Cr(CO)_5S$ species is formed in less than 50 ps in both THF and cyclohexane solutions [10].

The room-temperature 50 ps transient absorption spectrum of $Cr(CO)_6$ in methanol and cyclohexane has also been recorded (Fig. 1) [11]. Monitoring the transient absorption maximum (460 nm) of the photolysis of $Cr(CO)_6$ in methanol at intervals of 2 ps reveals a rapid rise for the $Cr(CO)_5$(MeOH) complex, remaining constant for up to 150 ps. Matrix photolysis investigations of $Cr(CO)_6$ using polarized light [6] support the proposal of Simon and Xie [11] that the photogenerated $Cr(CO)_5$ fragment undergoes isomerization (square pyramid → trigonal bipyramid → square pyramid interconversion), that electronic relaxation occurs prior to solvent coordination, and that the transient absorption rise in methanol reflects both $Cr(CO)_5$ isomerization and solvent coordination. Such an isomerization mechanism would give rise to a maximum of 67% production of $Cr(CO)_5S$. This agrees well with the photosubstitution quantum yield [2]. It is likely that the dissociation dynamics for $Cr(CO)_6$ in cyclohexane are rapid when compared with the time resolution of the experiment, and thus no risetime is observed [11]. A comparison of the results for $Cr(CO)_6$ in methanol and cyclohexane suggests that the risetime observed in methanol corresponds to the time associated with local solvent reorganization and coordination to the ground state fragment.

A preliminary study [12] of $W(CO)_6$ in perfluoromethylcyclohexane, cyclohexane, or in a paraffin oil claims the formation of $W(CO)_5S$ with a risetime of about 20 ps (Nd: YAG laser, 355 nm excitation); however, under the conditions used (laser pulse width, ca. 30–40 ps [13–15]) transient formation (ESA at ca. 470 nm) is pulse limited and no solvent dependence could therefore be delineated. The nature of the transient must be ascertained by other techniques and subpicosecond spectroscopy might yet unravel the formation kinetics of these solvatopentacarbonyl species. Also, because a high-power laser was utilized, multiphotonic events must not be discounted (see later).

Bernstein et al. [16] have employed photoacoustic calorimetry to determine the heat of reaction for the photoelimination of CO from $Cr(CO)_6$, $Mo(CO)_6$ and $W(CO)_6$ in ethanol and cyclohexane. Pulsed laser sources (25 ps pulses, 355 nm excitation) and high speed detection systems have permitted photocalorimetric studies of short-lived transient molecules with microsecond lifetimes.

Assuming that the initial absorbing state is the parent hexacarbonyl $M(CO)_6$, the terminal state is a "pentacarbonyl" species of uncertain structure, and the quantum yield for transformation between the initial and terminal states (i.e. the primary photodissociation of $M(CO)_6$) is 1.0. The photodissociation energies in both ethanol and cyclohexane are as follows: $Cr(CO)_6$, $\Delta H = 37 \pm 5$ kcal mol^{-1}; $Mo(CO)_6$, $\Delta H = 34 \pm 5$ kcal mol^{-1}; $W(CO)_6$, $\Delta H = 38 \pm 5$ kcal mol^{-1} [11(a)]. The near-identical results in the two solvents suggest negligible solvent effects. Moreover, these enthalpy data are in accord with bond energy estimates derived from kinetic data on thermal reactions [17].

C. SPECTROSCOPY OF METAL COMPLEXES WITH MONODENTATE LIGANDS

(i) Chromium(III)

The photochemical behavior of chromium(III) complexes can be understood in terms of excited state properties obtained by spectroscopic and photophysical measurements. For the most part, such measurements involve emission quantum yields and emission lifetimes quantified by temperature, wavelength, medium and environmental dependences, as well as by sensitization and quenching experiments. Early endeavors in the study of chromium(III) photochemistry established that either fluorescence or phosphorescence or both can occur. Generally, the observed fluorescence is broad, structureless and significantly Stokes shifted to the red, which is compatible with the quartet Q_1^0 $(t_{2g})^2(e_g)^1$ excited state configuration. Phosphorescence is a relatively long-lived, structured, narrow-band emission

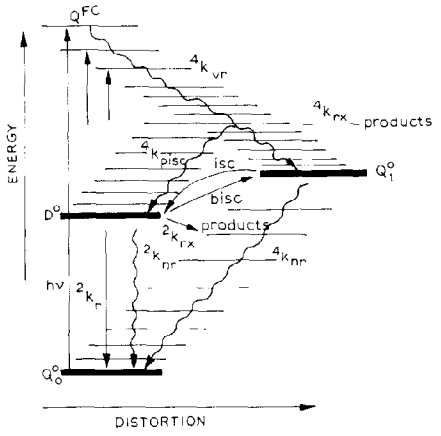

Fig. 2. Potential energy diagram and kinetic scheme for chromium(III) complexes.

with a small Stokes shift, compatible with the doublet D^0 $(t_{2g})^3(e_g)^0$ excited state configuration. The type of emission is closely linked to the quartet–doublet spacing, which is dependent on overall ligand-field strength. A potential energy diagram and kinetic scheme for chromium(III) is depicted in Fig. 2. While the doublet D^0 state of several chromium(III) complexes has been extensively characterized, far less is known about the quartet manifold. Kemp [18] and Kirk [19] have reviewed the photochemistry and photophysics of chromium(III) coordination complexes. Picosecond time resolution should make it possible to determine the role of the excited quartet state, Q_1^0, in the photochemistry of these complexes.

Transient absorption spectra of aqueous $Cr(NCS)_6^{3-}$, *trans*-$Cr(NH_3)_2(NCS)_4^-$ and *trans*-$Cr(en)_2(NCS)_2^+$ obtained by picosecond laser excitation [20,21] are identical to those obtained by nanosecond kinetic spectroscopy [22,23]. The risetimes of the transient absorbance in H_2O and D_2O are given in Table 1; they are independent of the probe wavelength and are longer than the value of less than 10 ps cited earlier [20]. The transient is the lowest doublet excited state D^0 [21] on the basis of the close similarity in decay times of excited state absorption and the decay time of phosphorescence intensity in *trans*-$Cr(NH_3)_2(NCS)_4^-$ at low temperature [24]. The lifetime would be expected to be dependent on the energy gap between the minima of the doublet D^0 and quartet Q_1^0 potential energy surfaces if the ESA rise reflected intersystem crossing (isc) from the vibrationally-equilibrated quartet state to the doublet state. Since the risetimes do not vary appreciably amongst the complexes, any dependence on $10Dq$ is ruled out. However, competition between intersystem crossing (k_{isc}) and vibrational relaxation

TABLE 1

Risetimes for the transient absorbance of some chromium(III) complexes [a]

Complex	Risetime (ps)	
	H_2O	D_2O
$Cr(NCS)_6^{3-}$	16 ± 2	12 ± 6
trans-$Cr(NH_3)_2(NCS)_4^-$	22 ± 2	11 ± 2
trans-$Cr(en)_2(NCS)_2^+$	16 ± 3	24 ± 2

[a] Ref. 21.

could occur, wherein the risetime would reflect a combination of intersystem crossing from Q_1^0 to D^0 and relaxation within the doublet manifold from the vibrational level isoenergetic with a Franck–Condon state Q_{FC} produced in the excited quartet at the laser pulse energy (530 nm). The observed lifetime need not be dependent on $10Dq$ if intersystem crossing is comparable with or faster than vibrational relaxation. A somewhat similar interpretation has been given by Gutierrez and Adamson [23] for *trans*-$Cr(NH_3)_2(NCS)_4^-$. As such, the lifetime τ may very well depend on the energy of the Franck–Condon state in the expeced quartet manifold, Q_{FC}.

The data in Table 1 expose a small but real isotope effect for the risetimes of these transient absorptions. The expected increase in τ (reduction in the rate constant) is observed for *trans*-$Cr(en)_2(NCS)_2^+$ in D_2O, with the opposite seen for *trans*-$Cr(NH_3)_2(NCS)_4^-$ and $Cr(NCS)_6^{3-}$. Pyke and Windsor [21] suggest that the unexpected results may be due to a charge dependence as put forward for *trans*-$Cr(NH_3)_2(NCS)_4^-$ [22,25], *trans*-$Cr(en)_2(NCS)F^+$ [25], $Cr(NH_3)_5(NCS)^+$ and $Cr(NCS)_6^{3-}$ [22].

Rojas and Magde [26] have measured the time-resolved emission spectra of *trans*-$Cr(NH_3)_2(NCS)_4^-$ and *trans*-$Cr(NCS)_6^{3-}$ in aqueous solution at ambient temperatures employing the 514 nm line of an argon ion laser with 150 ps pulses and an instrument response time of 440 ps. The time-resolved emission spectrum of *trans*-$Cr(NH_3)_2(NCS)_4^-$ exhibits a rise in phosphorescence at 750 nm and a weak, broad emission in the region 700–800 nm (cf. Fig. 3). Kinetic measurements yield $\tau \approx 5.5 \pm 0.5$ ns, assigned to phosphorescence from the doublet D^0, while the lifetime of the short-lived component is estimated at less than 100 ps. The D^0 lifetime is somewhat shorter than that reported by Kang et al. [27], but agrees well with extrapolated values obtained from experiments performed at lower temperature [23,28]. The time-resolved emission spectrum of aqueous $Cr(NCS)_6^{3-}$ shows a phosphorescence rise at 775 nm and a weak, broad emission at 675–820 nm. The slow emission risetime is 1.65 ± 0.1 ns; the risetime of the fast component is less than 100 ps. On the basis of its kinetic and spectral

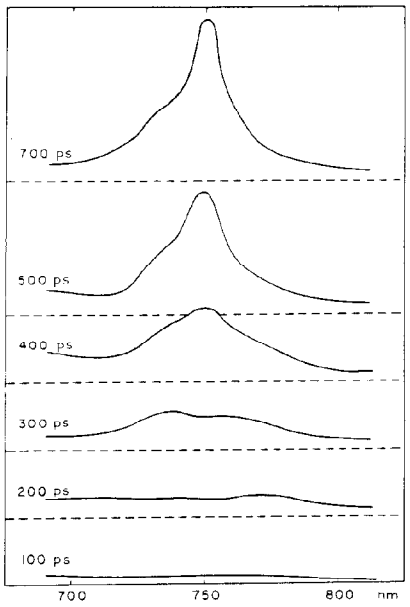

Fig. 3. Time-resolved emission spectra of $Cr(NH_3)_2(NCS)_4^-$ (from ref. 26).

behavior, the latter arises from prompt fluorescence; the slow component is due to phosphorescence possibly accompanied by thermally activated delayed fluorescence.

Transient absorption spectra of $Cr(NCS)_6^{3-}$, *trans*-$Cr(NH_3)_2(NCS)_4^-$, and *trans*-$Cr(en)_2(NCS)_2^+$ have been recorded in dimethylformamide (DMF), acetone, water, CH_3CN, D_2O and ethanol. The results have been analyzed in terms of the rate constants associated with doublet and quartet excited states [29]. The excited state absorption risetimes for *trans*-$Cr(NH_3)_2(NCS)_4^-$ and *trans*-$Cr(en)_2(NCS)_2^+$ are fastest in hydroxylic solvents and slowest in non-hydroxylic media; the data are presented in Table 2. The transients are assigned to excited state absorption from the doublet state D^0. Hollebone et al. [30] have described a model in which the photochemistry and intersystem crossing compete with vibrational relaxation and redistribution. The photochemical and photophysical behavior of a system is governed by population and decay on a specific nuclear coordinate. Those solvents capable of hydrogen bonding to the ligands might possibly couple to vibrational coordinates which are active in the intersystem crossing process. The solvent dependence shown by *trans*-$Cr(en)_2(NCS)_2^+$, *trans*-$Cr(NH_3)_2(NCS)_4^-$ and $Cr(NCS)_6^{3-}$ is consistent with the concept that hydrogen bonding is an important influence on the in-

TABLE 2

Excited state absorption results for chromium(III) complexes [a]

Complex	Solvent	λ_{max} (nm) [b]	Risetime (ps)
trans-$Cr(NH_3)_2(NCS)_4^-$	CH_3CN	533	18
	DMF	531	29
	CH_3COCH_3	530	27
	CH_3CH_2OH	530	8
	D_2O	510	6
	H_2O	510	< 6
trans-$Cr(en)_2(NCS)_2^+$	CH_3CN	558, 456	15
	H_2O	530	9
$Cr(NCS)_6^{3-}$	CH_3CN	516	5
	DMF	520	10
	H_2O	520	11
	65% glycerol–H_2O	516	6

[a] Ref. 29. [b] Absorption maxima of transient.

tersystem crossing rate [29]. However, further experimental evidence is required in order to verify the general applicability of this model to these systems.

Recently, Rojas et al. [31] employed picosecond laser spectroscopic techniques to examine the transient spectral features of *trans*-$Cr(NH_3)_2(NCS)_4^-$, $Cr(NCS)_6^{3-}$, $Cr(acac)_3$, $Cr(en)_3^{3+}$, $Cr(bpy)_3^{3+}$ and $Cr(phen)_3^{3+}$ (acac = acetylacetonate; en = ethylenediamine; bpy = 2,2′-bipyridine; phen = 1,10-phenanthroline) complexes as a function of excitation wavelength (314, 585 and 628 nm), solvent (H_2O, CH_3CN, DMF, acetone, methanol and dimethyl sulphoxide (DMSO), different apparatus and varying procedures. In the transient spectra (340–750 nm) of *trans*-$Cr(NH_3)_2(NCS)_4^-$ and $Cr(NCS)_6^{3-}$, instantaneous (< 1 ps) transient absorption is observed from weak photolysis pulses (< 1 nJ) at high repetition rates (82 MHz) to moderate energy pulses (30–200 μJ) at moderate repetition rates (10 Hz). Similarly, prompt absorption occurs in aqueous as in organic media. They found no evidence of the "slow" risetimes reported earlier. Both complexes in aqueous solution show a prominent induced absorption at 555 nm, weaker signals at 620 nm, and no measurable transient events at 680 nm. In accordance with previous reports, the transient spectral features after 2–4 ps are assigned [31] to absorption by the lowest doublet state D^0. The induced absorption decaying in 1–3 ps and observed only with 628 nm excitation may be associated with an initially populated quartet energy level, not necessarily in a thermally relaxed state. The absence of light-induced absorption upon 314 nm excitation is taken to mean that such excitation into a higher quartet state (or into

the lowest quartet manifold with a large excess of vibrational energy) gives rise to more efficient intersystem crossing to the doublet state. However, the observed presence of an artifact affiliated with the solvent blank raises questions about the nature of this induced absorption. Further, the strength of any correlation between this study and prior ones rests with the inability to produce 530 nm excitation as used in previous investigations. Several changes are not expected in excited state behavior when the excitation wavelength is changed, at least not for excitation into the same electronic state. However, chromium(III) photochemistry may be an exception [30]. Rojas et al. [31] suggest another possibility for their results. Transient absorption from the doublet state D^0 appears (i) immediately (< 1 ps) on excitation at 314 nm, (ii) after a longer delay (up to 20 ps and solvent dependent) on 585 nm excitation, and (iii) is accompanied by an additional short transient due to the quartet state for 628 nm excitation. This hypothesis lends credence to excitation wavelength dependences. However, the identity of the transient absorption for these chromium(III) complexes awaits further clarification.

(ii) Ruthenium(II)

Pentaammineruthenium(II) complexes with aromatic *N*-heterocyclic ligands (L), $Ru(NH_3)_5L^{2+}$, (i) allow extensive investigations of inorganic photochemical reaction mechanisms [32,33], (ii) serve as building blocks for binuclear complexes for which intermolecular electron-transfer kinetics and mechanisms can be obtained [34,35], and (iii) show similarities in their excited state manifolds to those of polypyridineruthenium(II) complexes [36].

The visible absorption spectra of $Ru(NH_3)_5L^{2+}$ are dominated by intense metal-to-ligand charge-transfer (MLCT) bands sensitive to the nature of L and to the solvent [37]. Visible-light excitation of $Ru(NH_3)_5L^{2+}$ yields photosubstitution processes characteristic of ligand-field photochemistry [32]. Malouf and Ford [38] propose an "excited state tuning" model in which those complexes with MLCT absorption maxima at 460 nm or below possess lowest energy excited states of ligand-field character, while those complexes with MLCT absorption maxima above 460 nm have lowest energy excited states of MLCT character. However, the lack of sufficient spectroscopic and photophysical data precludes quantitative confirmation of the "excited state tuning" model.

Winkler et al. [39] have used picosecond transient absorption spectroscopy to obtain excited state lifetimes and difference spectra, as well as electrochemical and spectral data and photoaquation quantum yields under continuous (CW) and picosecond laser photolysis for $[Ru(NH_3)_5L]X_2$ (L =

TABLE 3

Lifetimes and assignments of transients produced upon picosecond laser excitation [a]

Complex	Lifetime (ps)	Assignment
$Ru(trpy)_2^{2+}$	250	MLCT
$Ru(NH_3)_5L^{2+}$		
L = py	$\ll 20$ [b]	MLCT
4-C_6H_5py	~ 450	MLCT
isn	140	–
pz	225	MLCT
4,4′-bpy	< 36, 230 [b]	MLCT
	60 [b,c]	MLCT
4,4′-bpyH$^+$	< 30 [b]	MLCT
pzH^+	< 30	MLCT
$pzCH_3^+$	< 30	MLCT

[a] Ref. 39. [b] Permanent photoproduct also observed. [c] In CH_3CN solvent.

pyridine (py), pyrazine (pz), 4-phenylpyridine (4-C_6H_5py), isonicotinamide (isn), 4-acetylpyridine (4-acpy), 4,4′-bipyridine (4,4′-bpy); X = PF_6^-, ClO_4^-, $CF_3SO_3^-$) and $Ru(trpy)_2^{2+}$ (trpy = 2,2′,2″-terpyridine) in aqueous media. For each complex, a pulse of about 20 ps at 532 nm (except for L = py, where $\lambda_{exc} = 355$ nm) results in a transient absorption for which lifetimes range from $\leqslant 20$ to 250 ps; these are listed in Table 3.

The good correlation between the transient spectra of $Ru(trpy)_2^{2+}$ and $Ru(bpy)_3^{2+}$ (bpy = 2,2′-bipyridine) suggests an MLCT assignment to the 250 ps transient observed for the trpy complex. MLCT excited states of $Ru(bpy)_3^{2+}$ have also been characterized [40] in terms of the $M^{III}L^-$ chromophore with L^- intraligand (IL or LC or LL) transitions providing a distinctive feature. The MLCT state of the $Ru(NH_3)_5L^{2+}$ complexes is also modeled as $Ru^{III}(NH_3)_5(L^-)^{2+}$, and the MLCT state should reveal absorption(s) due to L^-. Comparison of ground state absorption spectra of protonated L generated by pulse radiolysis with transient difference spectra of $Ru(NH_3)_5(L^-)^{2+}$ (or $Ru(NH_3)_5(LH)^{3+}$) lends credence to the assignment of the first transient produced with 532 nm excitation as MLCT states. Two transients ($\tau \leqslant 36$ and 230 ps) are observed [39] for $Ru(NH_3)_5$(4,4′-bpy)$^{2+}$ (see Fig. 4), with the process with $\tau \leqslant 36$ ps ascribed to solvent relaxation of the Franck–Condon MLCT state, to intersystem crossing (singlet → triplet), or to a conformational change in the 4,4′-bpy ligand. Ligand-field excited states of the $Ru(NH_3)_5L^{2+}$ complexes are not directly observed, probably because they are too short lived compared with the MLCT states. Winkler et al. [39], however, are concerned with the susceptibility of these complexes to multiphoton-induced photochemistry, particu-

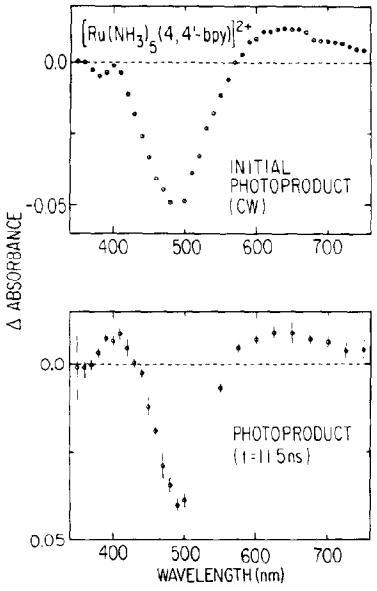

Fig. 4. Comparison of difference spectra of $Ru(NH_3)_5(4,4'\text{-bpy})^{2+}$ in water after CW photoexcitation above 500 nm (top) and after 532 nm pulsed laser excitation (bottom) taken at a delay time of 11.5 ns (from ref. 39).

larly for those complexes exhibiting wavelength-dependent photolytic behavior.

(iii) Rhodium(III)

Luminescence lifetimes of the rhodium(III) ammine complexes RhL_5X^{2+} ($L = NH_3$, ND_3; $X = Cl$, Br) in fluid media at ambient temperature have been determined by nanosecond pulsed laser techniques [41]. A combination of these measurements and quantum yield measurements affords calculation of first-order rate constants for the major deactivation pathways from the luminescent ligand-field (LF) excited state triplet. LF excitation of complexes of the type $Rh(NH_3)_5X^{2+}$ generally leads to labilization of coordinated ligands, with quantum yields dependent on the nature of the ligand labilized, on the reaction medium and on the balance of the first coordination sphere. Wavelength dependence and sensitization studies on $Rh(NH_3)_5X^{2+}$ show that LF excitation is followed by efficient internal conversion ($\phi_{isc} \approx 1$) or intersystem crossing ($\phi_{isc} \approx 1$) to a common set of states responsible for the bulk of the photoreaction [42]. These states are

thought to be the lowest energy LF triplet excited states and those states in thermal equilibrium with the lowest energy excited states [41,43].

The effects arising from slight changes in the coordination sphere of $Rh(NH_3)_5Br^{2+}$ and $Rh(NH_3)_4Br_2^+$ have been probed at ambient temperature in 10^{-3} M $HClO_4$(aq) using subnanosecond laser spectroscopic methods (200 ps pulses, 458 nm excitation) [44]. Using eqn. (2a)

$$k_i = \phi_i/\tau \tag{2a}$$

and

$$\phi_i = k_i/(k_{NH_3} + k_{X^-} + k_r + k_{nr}) \tag{2b}$$

where ϕ_i is the quantum yield for an excited state process i, and k_{NH_3}, k_{X^-}, and k_{nr} are the excited state rate constants for aquation of NH_3, aquation of X^-, radiative deactivation and non-radiative deactivation respectively, and τ is the luminescence lifetime, values of k_{Br^-}, k_{NH_3} and k_{nr} can be estimated for $Rh(NH_3)_5Br^{2+}$ and *cis*- and *trans*-$Rh(NH_3)_4Br_2^+$. Results show that the introduction of an additional Br^- into the coordination sphere accelerates Br^- labilization from the excited state regardless of the stereochemical position relative to the leaving Br^- group. The excited state substitution reaction is stereomobile, proceeding via a limiting dissociative mechanism [45]. The rate of NH_3 photolabilization (k_{NH_3}) for *cis*-$Rh(NH_3)_4Br_2^+$ is larger than that for $Rh(NH_3)_5Br^{2+}$; this is attributed to greater stabilization of the ligand labilization pathway transition state by Br^- in the coordination sphere, relative to NH_3 in the same site [44]. Utilizing the excited state bond index model of Vanquickenborne and Ceulemans [46], which assumes a dissociative mechanism, Ford and coworkers [44] propose that the lowest LF excited state of $Rh(NH_3)_5Br^{2+}$ should labilize the NH_3 *trans* to Br^-, that of *cis*-$Rh(NH_3)_4Br_2^+$ should labilize an NH_3 *trans* to Br^- or a Br^- about equally, and that of *trans*-$Rh(NH_3)_4Br_2^+$ should labilize Br^-.

The same nanosecond laser system was employed to determine luminescence lifetimes of several rhodium(III) haloammine complexes; the data are collected in Table 4 [47]. Under the experimental conditions used, two emission components were distinguished. One is the slow emission ($\tau_P > 1$ ns) which is assigned to LF phosphorescence; the other is a faster decay centered at shorter wavelengths and shows no detectable temperature dependence. The observation that the fraction of total emission associated with the fast decay increases at shorter wavelengths, while the fraction of total emission associated with the slow decay component increases at longer wavelengths, implies that the fast component arises from a higher energy state or group of states. Thus the fast emission component is thought to be fluorescence from initially populated singlet LF excited states [47].

TABLE 4

Luminescence lifetimes of some rhodium(III) complexes in dilute $HClO_4$ (298 K) [a]

Complex	τ_F (ps)	τ_P (ns)
$Rh(NH_3)_5Br^{2+}$	220	13.0 ± 0.4
trans-$Rh(NH_3)_4Br_2^+$	90	1.5 ± 0.1
cis-$Rh(NH_3)_4Br_2^+$	60	1.0 ± 0.1
trans-$Rh(NH_3)_4Cl_2^+$	90	1.8 ± 0.3
cis-$Rh(NH_3)_4Cl_2^+$	70	1.3 ± 0.3
trans-$Rh(NH_3)_4(H_2O)Br^{2+}$	100	1.7 ± 0.6
cis-$Rh(NH_3)_4(H_2O)Br^{2+}$	50	1.6 ± 0.6
trans-$Rh(NH_3)_4(H_2O)Cl^{2+}$	100	2.2 ± 0.6
cis-$Rh(NH_3)_4(H_2O)Cl^{2+}$	60	2.4 ± 0.6

[a] Ref. 47.

(iv) Cobalt(III)

The complexes $Co(NH_3)_5Cl^{2+}$, *cis*- and *trans*-$Co(en)_2Cl_2^+$, *trans*-$Co(en)_2(NO_2)_2^+$, and *cis*-$Co(en)_2(NCS)Cl^+$ have been examined with 355 nm pulsed-laser excitation (mode-locked Nd : YAG) [13]. Transient absorption was only observed for the dinitro and isothiocyanato complexes; in the latter case, a transient forms and decays in 40 ps or less (pulse limited) in favor of a lower energy band at about 605 nm. For the dinitro complex, the preliminary transient is not well defined but there is again a longer-lived transient with $\tau = 150 \pm 30$ ps. The visible transient absorptions were assigned [13] to a transition from the lowest ligand-field triplet ($^3T_{2g}$ in O_h microsymmetry) to a ligand-based acceptor π^* orbital.

D. SPECTROSCOPY OF METAL COMPLEXES WITH BIDENTATE LIGANDS

(i) Chromium(III)

In efforts to understand the role of excited states, Linck et al. [48] have investigated several chromium(III) complexes containing ethylenediamine (en) and 1,3-propanediamine (tn) ligands by picosecond laser spectroscopy with a mode-locked argon ion laser (150 ps pulses), an excitation wavelength of 514.5 nm, an instrument response time of 12.2 ns, and iterative deconvolutions. The strategy involved directly measuring excited state lifetimes for complexes of slightly varying structure in order to test the correlation between a lifetime-controlling process and the relevant energy barrier to back intersystem crossing (see k_{bisc} in Fig. 2). A change in molecular

TABLE 5

Photochemical data for chromium(III) complexes with en and tn ligands [a]

Complex		τ (ns) [b]	Emission λ_{max} (nm)	10^{-3} E (cm^{-1}) [c]
A	*trans*-$Cr(en)_2(NCS)_2^+$	4400 ±300	730	19.78
B	*trans*-$Cr(tn)_2(NCS)_2^+$	1500 ±100	725	19.63
C	*trans*-$Cr(en)_2F_2^+$	1280 ±100	Broad	19.03
D	*trans*-$Cr(en)_2(NCS)F^+$	325 ± 30	723	19.44
E	*cis*-$Cr(tn)_2(NCS)(H_2O)^{2+}$	30 ± 6	696	19.24
F	*trans*-$Cr(en)_2(F)(H_2O)^{2+}$	25 ± 6	770	18.98
G	*cis*-$Cr(en)_2(NCS)(H_2O)^{2+}$	20 ± 4	703	19.40
H	*trans*-$Cr(en)_2(NCS)(H_2O)^{2+}$	12 ± 4	705	19.30
I	*trans*-$Cr(tn)_2(NCS)(H_2O)^{2+}$	10 ± 2	699	19.15
J	*cis*-$Cr(tn)_2(H_2O)_2^{3+}$	3.5 ± 0.5	675	18.80
K	*trans*-$Cr(tn)_2(H_2O)_2^{3+}$	3.0 ± 0.3	672	18.67
L	*trans*-$Cr(NH_3)_4(NCS)(H_2O)^{2+}$	2.5 ± 0.5	694	18.98
M	*cis*-$Cr(en)_2(H_2O)_2^{3+}$	2.4 ± 0.4	680	18.96
N	$Cr(H_2O)_6^{3+}$	1.8 ± 0.3	–	15.83
O	*cis*-$Cr(tn)_2(Cl)(H_2O)^{2+}$	1.3 ± 0.2	688	18.10
P	*trans*-$Cr(en)_2(NCS)Br^{2+}$	1.9 ± 0.3	–	18.20

[a] Ref. 48. [b] In aqueous solution at ambient temperature. [c] The difference between ground state and the calculated energy of the lowest lying quartet state at ground state internuclear distances.

structure affords a lifetime change of three orders of magnitude, as indicated in Table 5. Also, (i) for the *trans*-diisothiocyanato complexes A and B, the tn complex has a slightly smaller lifetime than the en complex, whereas similar lifetimes are observed for the *cis*- and *trans*-thiocyanatoaquo complexes E, G, H and I; (ii) the *trans* complexes have shorter lifetimes than comparable *cis* complexes; (iii) a shorter lifetime is observed for the monodentate amine complex L than for complexes H and I containing the bidentate en and tn ligands. Further, a slight trend of increasing decomposition rate is evident as the ligands vary from en to tn to NH_3. In efforts to discern whether chemical reaction or back intersystem crossing dictates the doublet state lifetime, the authors [48] correlated the calculated energy of the first spin-allowed transition (cf. Table 5, E) with the lifetime data. In the energy region $(18.8–19.8) \times 10^3\ cm^{-1}$, larger values in the energy difference lead to smaller rate constants for doublet excited state relaxation. It appears that back intersystem crossing is the predominant decay process for the doublet state of these complexes, and that this model may account for the trends in lifetime data as well as for the trends in the lifetime–energy relationship [48].

(ii) Rhodium(III)

Studies similar to those of $Rh(NH_3)_5Br^{2+}$ and *cis*- and *trans*-$Rh(NH_3)_4Br_2^+$ [44] have been carried out for $Rh(tn)_2X_2^+$ and $Rh(tn)_2(L)X^{2+}$ (X = Cl, Br; L = H_2O, OH) in dilute aqueous solution at 298 K. Ligand-field excitation of *cis*- and *trans*-$Rh(tn)_2X_2^+$ in acidic aqueous media leads to halide photoaquation with quantum yields of 0.080 (*trans*-$Rh(tn)_2Cl_2^+$), 0.055 (*trans*-$Rh(tn)_2Br_2^+$), 0.56 (*cis*-$Rh(tn)_2Cl_2^+$), and 0.64 (*cis*-$Rh(tn)_2Br_2^+$) mol einstein^{-1} [49]. No amine photoaquation occurs for any of the tn complexes. The phosphorescence lifetimes (458 nm excitation, 200 ps pulses) are as follows (in 10^{-3} M $HClO_4$ at 298 K): for *trans*-$Rh(tn)_2Cl_2^+$, 1.4 ± 0.1 ns; for *cis*-$Rh(tn)_2Cl_2^+$, 0.9 ± 0.1 ns; for *trans*-$Rh(tn)_2Br_2^+$, 0.67 ± 0.07 ns; and for *cis*-$Rh(tn)_2Br_2^+$, 0.30 ± 0.05 ns. For $Rh(NH_3)_4X_2^+$ complexes, an analysis of the luminescence decay profiles of $Rh(tn)_2X_2^+$ reveals two emission components: a short-lived component ($\tau < 100$ ps) and a longer-lived component (nanosecond time scale) [49].

Ligand-field excitation of *cis*- and *trans*-$Rh(en)_2X_2^+$ (X = Cl, Br) in acidic solution at 295 K leads to halide photoaquation yielding $Rh(en)_2(H_2O)X^{2+}$. Phosphorescence lifetimes in 10^{-3} M $HClO_4$(aq) at 298 K are as follows: for *trans*-$Rh(en)_2Cl_2^+$, 2.2 ± 0.4 ns; for *cis*-$Rh(en)_2Cl_2^+$, 2.5 ± 0.4 ns; for *trans*-$Rh(en)_2Br_2^+$, 2.2 ± 0.2 ns; and for *cis*-$Rh(en)_2Br_2^+$, 2.5 ± 0.2 ns. The emission decay curves are described by a single-exponential function convoluted with the excitation function. By analogy with $Rh(NH_3)_4X_2^+$ and $Rh(tn)_2X_2^+$ complexes, the emission is assigned to phosphorescence from the lowest energy LF excited state triplet [50].

(iii) Nickel(II)

Preliminary studies [51] show that the planar dibromo-1,2-(diphenylphosphinoethane)nickel(II) complex, Ni(dpe)Br_2, in CH_3CN is slightly dissociated (eqn. (3)):

$$Ni(dpe)Br_2 \overset{K}{\rightleftharpoons} Ni(dpe)Br(S)^+ + Br(S)^- \qquad (3)$$

where $K < 10^{-6}$ mol dm^{-3} and (S) denotes solvation by CH_3CN. An ionic transient species is observed within the 30 ns risetime of the laser pulse during flash photolysis. The transient decays with a time constant of 12–35 μs and varies with the Ni(dpe)Br_2 concentration. The same species is formed [52] in both CH_3CN and CH_2Cl_2 upon 530 nm excitation with 10 ps pulses from an Nd : glass mode-locked laser (Fig. 5). This species is likely to be a tetrahedrally distorted excited state of Ni(dpe)Br_2, inasmuch as the difference spectra lie in the region characteristic of tetrahedral complexes. Moreover, previous analyses of nickel(II) complexes using angular overlap

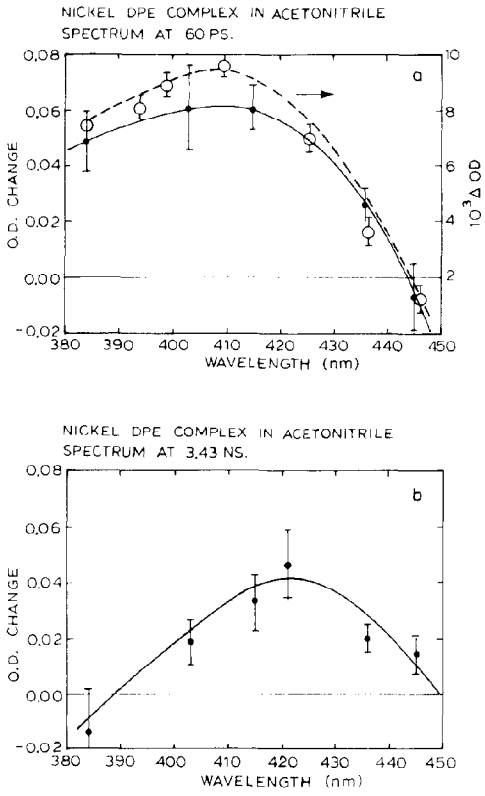

Fig. 5. Transient absorption spectra of $Ni(dpe)Br_2$ in CH_3CN at (a) 60 ps and (b) 3.4 ns after the 10 ps laser excitation pulse. The broken line spectrum in (a) refers to the transient spectrum in CH_2Cl_2 with a 30 ns laser pulse (from ref. 52).

models [53] and spectroscopic studies [54] support a tetrahedral structure and a triplet spin state for the transient.

In CH_2Cl_2, transient absorption appears promptly and decays with $\tau \approx 25$ ns at 294 K. This transient probably decays via triplet $\rightarrow$ singlet intersystem crossing with $k \approx 4 \times 10^7\ s^{-1}$. In CH_3CN, the transient absorption decays with $\tau \approx 0.9$ ns into a longer-lived species, which decays in microsecond time and confirms the observations of Campbell [51]. The lifetime of 0.9 ns reflects the formation of the ionic species $Ni(dpe)Br(S)^+$ (see eqn. (3)) via nucleophilic solvent attack on the triplet excited state, formed upon picosecond excitation (eqns. (4) and (5)):

$$Ni(dpe)Br_2 \xrightarrow{h\nu} Ni(dpe)Br_2^* \tag{4}$$

$$Ni(dpe)Br_2^* + S \rightarrow Ni(dpe)(Br)(S)^+ + Br(S)^- \tag{5}$$

Picosecond examination of $Ni(mnt)_2^{2-}$ and $Pt(mnt)_2^{2-}$ complexes in CH_3CN, where mnt is maleonitriledithiolate $(S_2C_2(CN)_2^{2-}$, with delay times between 20 ps and 10 ns, shows that the initially populated state rapidly partitions between a low lying singlet and triplet state [15]. The singlet decay time for the platinum species is 5 ns compared with about 50 ps for the nickel analog. Added water quenches the triplet state from $\tau > 10$ ns to $\tau \approx 3$ ns.

(iv) Polypyridine complexes

Polypyridine complexes of chromium, iron, ruthenium, osmium, rhodium and iridium have been the subjects of extensive photochemical investigations. Those of chromium(III) and ruthenium(II) have been utilized for studies in photochemical energy storage as their lowest energy excited states are relatively long lived and thus capable of exploring a variety of electron transfer reactions.

(a) Vanadium(II)

Shah and Maverick [55] have examined vanadium(II) polypyridine complexes in an effort to combine the functions of sensitizer and multielectron redox agent in a single molecule, thus eliminating the necessity of additional homogeneous or heterogeneous catalysts to achieve significant quantum yields for energy storage (see for example ref. 56). In particular, $V(bpy)_3^{2+}$ and $V(phen)_3^{2+}$ were investigated by picosecond flash photolysis methods (35 ps pulses at 355 and/or 532 nm), as well as by microsecond and nanosecond techniques. No signals attributable to vanadium(II) species are seen in nanosecond time. Picosecond transient difference spectra of $V(bpy)_3^{2+}$ and $V(phen)_3^{2+}$ in ethanol (532 nm excitation) show GSB from 550 to 690 nm and a broad ESA band above 700 nm (Fig. 6). Additionally, transient absorption is observed at 490–550 nm for $V(phen)_3^{2+}$ upon 355 nm excitation. Excited state lifetimes for $V(phen)_3^{2+}$ and $V(bpy)_3^{2+}$ are 1.8 ± 0.1 ns and 0.5 ± 0.1 ns respectively.

Assuming octahedral microsymmetry for both complexes, König and Herzog [57] have assigned the lowest energy spin-allowed *d–d* transition to the $^4A_2 \rightarrow {}^4T_2$ transition at about 650 nm; a strong contribution from MLCT transitions is acknowledged owing to the high intensity of these bands. The lowest energy electronic absorption bands in $V(bpy)_3^{2+}$ and $V(phen)_3^{2+}$ occur at 660 nm and 640 nm respectively [55]. Both *d–d* and MLCT transitions are thought to contribute to these absorptions, and the resulting excited states do not mix extensively. Thus the lowest energy excited states are thought to be either an $^2E/^2T$ doublet or an MLCT

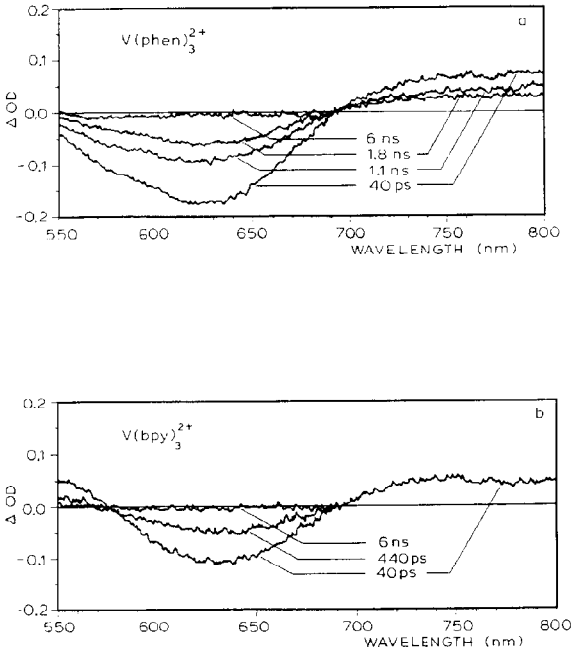

Fig. 6. Picosecond transient difference spectra in ethanol solution for (A) $V(phen)_3^{2+}$ and for (B) $V(bpy)_3^{2+}$ with 532 nm excitation and 35 ps pulses (from ref. 55).

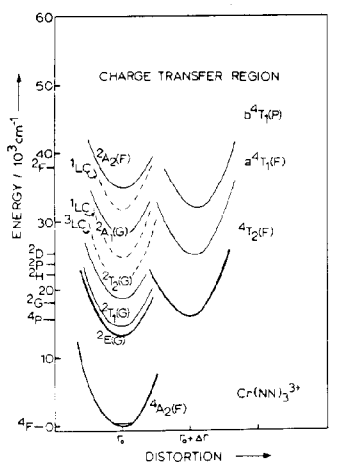

Fig. 7. Qualitative energy level diagram as a function of a distortion coordinate for chromium(III) polypyridine complexes (from ref. 71).

quartet state. The excited state lifetime is smaller for the bpy complex than for the phen complex, analogous to findings in chromium(III) species [58].

(b) Chromium(III)

A perpetual controversy in the photochemistry and photophysics of chromium(III) complexes encompasses the specific role(s) played by the excited quartet and excited doublet states in defining the photochemical behavior. The case of chromium(III) polypyridyl complexes provides an excellent case study whereby mechanistic details of energy redistribution, dissipation and relaxation evolve as more and more data become available from various techniques to unravel the role(s) of excited states in the photochemical and photophysical behavior of these complexes. That the behavior can be complicated is seen on considering the variety and multitude of states involved in these chromium(III) complexes (cf. Fig. 7).

$^4A_2 \xrightarrow{h\nu} {}^4T_2$	(excitation, I_a)
$^4T_2 \rightarrow {}^4A_2$	(non-radiative decay, $^4k_{nr}$)
$^4T_2 \rightarrow {}^2T_1/{}^2E$	(intersystem crossing, $^4k_{isc}$)
$^4T_2 \xrightarrow{H_2O}$ photoaquation	(reactive decay, $^4k_{rx}$)
$^2T_1/{}^2E \rightarrow {}^4A_2 + h\nu'$	(emission decay, ^2k_r)
$^2T_1/{}^2E \rightarrow {}^4A_2$	(non-radiative decay, $^2k_{nr}$)
$^2T_1/{}^2E \xrightarrow{^4A_2/Cl^-} {}^4A_2$	(ground state quenching, ^2k_g)
$^2T_1/{}^2E \xrightarrow{Q}$ quenching	(quenching modes, ^2k_q)
$^2T_1/{}^2E \xrightarrow{H_2O} Cr(NN)_3(H_2O)^{3+}$	(reactive decay, $^2k_{rx}$)
$Cr(NN)_3(H_2O)^{3+} \xrightarrow[H_2O]{H^+} {}^4A_2$	(decay of intermediate)
$Cr(NN)_3(H_2O)^{3+} \xrightarrow[H_2O]{H^+} Cr(NN)_2(H_2O)_2^{3+} + NNH^+$	(labilization of intermediate)
$Cr(NN)_3(H_2O)^{3+} \rightleftharpoons Cr(NN)_3(OH)^{2+} + H^+$	(deprotonation of intermediate)
$Cr(NN)_3(OH)^{2+} \xrightarrow{OH^-} Cr(NN)_2(OH)_2^+ + NN$	(labilization of deprotonated intermediate)

Scheme 1

For $Cr(bpy)_3^{3+}$, a photochemical model has evolved [59,60] to account for the experimental results obtained; this model is depicted in Scheme 1. The

vibrationally relaxed lowest doublet excited states ($^2T_1/^2E$) are populated by nearly quantitative intersystem crossing from the short-lived $^4T_2$ state with back intersystem crossing not being an important decay mode for the $^2T_2/^2E$ states [61]. The photoaquation of $Cr(bpy)_3^{3+}$ in alkaline aqueous media has been attributed to direct reaction from the $^2T_1/^2E$ states, and constitutes the quenchable part of the photoreaction. The unquenchable component of the photoreaction is believed to originate from the $^4T_2$ quartet state. Normalized data for (i) the quantum yield of reaction for the $^4T_2$ state, (ii) the quantum yield of reaction for the $^2T_1/^2E$ state, and (iii) the phosphorescence yield for $Cr(bpy)_3^{3+}$ reveal identical behavior as a function of wavelength of excitation [62]. Assuming Scheme 1 to be operative, the phosphorescence quantum yield and the reaction quantum yield of the quenchable component (i.e. from the doublet excited state) is expected to decrease at some appropriate wavelength corresponding to the potential surface of the quartet manifold crossing the potential surface of the $^2T_1/^2E$ (D^0) states (cf. Fig. 2). Further, no wavelength dependence (or a slight increase with increasing wavelength) is expected for the reaction quantum yield of the unquenchable component originating from the $^4T_2$ (Q_1^0) state. Serpone [62] has proposed that the wavelength dependence observed for the unquenchable component can be rationalized in terms of the unquenchable photoreaction originating from an unrelaxed level of the $^4T_2$ manifold. Temperature dependence studies of the reaction quantum yield of the unquenchable component yields $^4\Delta H_{rx} \approx 10$ kcal mol^{-1} and $^4\Delta S_{rx} \approx 13$ e.u. [61]. Direct probing of the $^4T_2$ state of chromium(III) polypyridyls was clearly imperative.

Population and Raman scattering of the ^2E and $^4T_2$ excited states of $Cr(bpy)_3^{3+}$ have been probed by Koningstein and coworkers [63]; an aqueous solution of the complex was exposed to radiation at 457.9 nm from a tunable pulsed (3.2 ns pulses) nitrogen laser and a CW fixed-wavelength laser. The lifetime of $(^4T_2)Cr(bpy)_3^{3+}$ was said to be about 10 ps from considerations of saturation effects, presumably observed for the ^2E state (CW laser) and for the $^4T_2$ state (pulsed laser). It should be pointed out that under pulsed flash photolysis excitation a secondary transient forms in aqueous media with a lifetime of several milliseconds, in addition to the ^2E state [64]. The formation of this secondary transient appears to have been overlooked, or its significance neglected [63]. The facile formation and relatively slow decay of the secondary transient preclude the possibility of saturating the ^2E state under steady state conditions by CW illumination. A re-examination of the time-resolved resonance Raman spectra of excited $Cr(bpy)_3^{3+}$ at pH 0 by Woodruff et al. [65], under conditions where formation of the secondary transient is negligible, shows that no illumination conditions can be achieved that might result in appreciable $^4T_2$ population

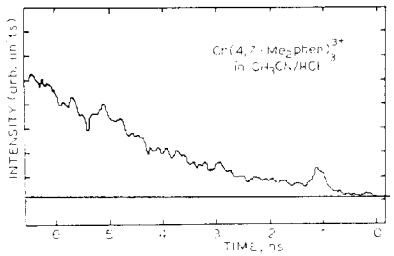

Fig. 8. Time evolution of the emission grow-in originating from D_0 states of Cr(4,7-Me_2phen)$_3^{3+}$ in CH_3CN–HCl(aq) (5% v/v) (from ref. 66).

with nanosecond excitation (7 ns pulse; Nd : YAG third harmonic irradiation, 354.7 nm). The pulsed excited spectra show saturation of the ^2E state. In the saturation absorption measurements carried out by Koningstein and coworkers [63], which purport to demonstrate CW saturation of the ^2E state, the observed positive transmission change (i.e. negative absorbance change) more probably arises from secondary transient formation; this may be the major steady state species produced under the conditions employed [65]. The earlier "$^4T_2$" time-resolved resonance Raman result [63] is more apt to be that for the (^2E)Cr(bpy)$_3^{3+}$ excited state species [65].

Luminescence spectroscopy (Nd : YAG laser; 355 nm excitation; about 30 ps full width at half-maximum (FWHM) excitation pulses) of Cr(bpy)$_3^{3+}$ and Cr(4,7-Me_2phen)$_3^{3+}$ (4,7-Me_2phen = 4,7-dimethyl-1,10-phenanthroline) in 1 M HCl(aq) reveals a slow grow-in of the luminescence from the $^2T_1/^2E$ state ($\tau_{rise} \approx 10$–20 ns) (Fig. 8) [66]. Transient absorption spectroscopy also showed a rapid increase in absorption in the 400–600 nm region within the integrated laser pulse (~ 30 ps), followed by a slower absorption rise to 12 ns [66]. The fast rise was attributed to the formation of the lowest quartet state, $^4T_2$, and the slower rise to formation of ^2E after populating the upper high energy states. The observations led to $k_{isc} \approx 1 \times 10^8$ s^{-1} (see Scheme 1 and Fig. 2) and a lifetime of 10 ± 4 ns for the lowest $^4T_2$ manifold of Cr(4,7-Me_2phen)$_3^{3+}$ using the Castelli and Forster model [67].

Kirk et al. [68] have questioned the results of Serpone et al. [66] with regard to the lack of observable fluorescence from the $^4T_2$ state, the possible presence of artifacts (e.g. filter emission, Raman effects), and the emission "concaves upward". Employing the same laser system, Kirk et al. [68] also examined the transient absorptions of Cr(bpy)$_3^{3+}$ in 0.05 M $HClO_4$ and of Cr(phen)$_3^{3+}$ in 0.003 M HCl. For both complexes, the transient absorbance rises with the integrated laser pulse, implying a risetime of 30 ps or less. After this rise, the absorbance remained constant out to 400 ps (bpy) and to 100 ps (phen). No reasons were given for not probing at longer delay times

[68]. They concluded that the excited state absorption rise of 30 ps or less results from formation of the $(^2E)Cr(NN)_3^{3+}$ species (NN = polypyridine). Nevertheless, it appears that the slow rise is not due to artifacts [69]. Subsequently, Serpone and Hoffman [69] put forward a model to account for the slow emission rise in $Cr(4,7\text{-}Me_2phen)_3^{3+}$ [66] inasmuch as the Castelli–Forster model was inappropriate since the Q_1^0 state in Fig. 2 is not populated. In the model, the initial population of an upper excited state within the excited quartet manifolds was thought to relax down the vibrational ladder in a few hundred picoseconds to attain an intermediate geometry. The relaxation process might be relatively slow because of displacement of solvent molecules and anions within the second coordination sphere as the complex proceeds along the distortion coordinate (cf. Fig. 2). However, this model was later revised (see below) as more data became available.

Rojas and Magde [70] and coworkers [31] also questioned the results and interpretations proposed by Serpone et al. [66] for chromium(III) polypyridyl complexes. They did agree, however, that the transient absorption seen by Serpone et al. [66] may well be that of the doublet state, and that the excited quartet LF state could have a transient absorption similar to that of the doublet such that one state might evolve into the other with little observable change. Employing low-power time-correlated photon-counting methods (340 nm excitation, 5–10 ps pulses), these authors [70] produced the complete phosphorescence rise and decay of $Cr(bpy)_3^{3+}$ and $Cr(phen)_3^{3+}$ in aqueous media (pH 4 and 1 M HCl). For both complexes, full emission intensity is achieved within $\ll 1$ ns. Deconvolution of the data indicated that phosphorescence from $Cr(NN)_3^{3+}$ appears in less than 100 ps. No many-nanosecond phosphorescence risetime was observed. It was acknowledged that perhaps transient absorption methods are not capable of distinguishing the doublet state from precursor states, and that the doublet and its phosphorescence "grow in" over tens of picoseconds. There were few differences in experimental conditions between the work of Rojas and Magde [70] and Serpone et al. [66], except perhaps the extreme difference in peak laser excitation power, which could account for the discrepant results between the two groups. Serpone et al. [66] employed 10^{17} photons incident on samples having 2×10^{15} absorbers; Rojas and Magde [70] used pulses with less than 10^8 photons. Thus the potential for multiphotonic events existed in the former work, but was not expected [66] without similar experiments with "softer" lasers.

A complete transient emission survey of several chromium(III) polypyridyl complexes by Serpone and Hoffman [71] followed. It revealed that 355 nm excitation (about 30 ps FWHM pulses) results in a fast emission component below 650 nm, which decays in about 50 ps (Figs. 9 and 10).

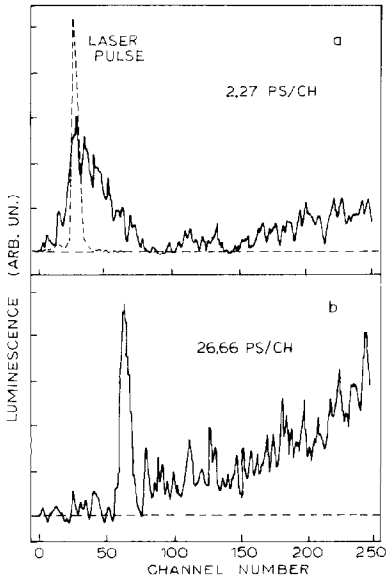

Fig. 9. Time-resolved emission from 355 nm excitation of $Cr(5,6\text{-}Me_2phen)_3^{3+}$ at two different streak speeds of the Streak camera: (A) time window, 568 ps, (B) time window, 6.7 ns (from ref. 71).

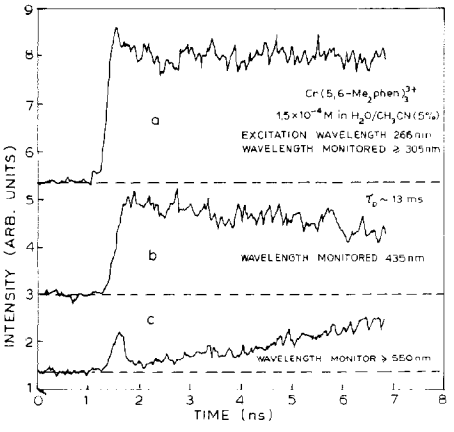

Fig. 10. Time-resolved transient emission from 266 nm laser excitation of $Cr(5,6\text{-}Me_2phen)_3^{3+}$ in CH_3CN–water (5% v/v). Plot A is the composite of plots B and C. From ref. 71.

This is observed [71] for $Cr(NN)_3^{3+}$ where NN = bpy, 4,4′-dimethyl-2,2′-bipyridine (4,4′-Me_2bpy), 4,4′-diphenyl-2,2′-bipyridine (4,4′-Ph_2bpy), phen, 5-chloro-1,10-phenanthroline (5-Clphen), 5-bromo-1,10-phenanthroline (5-Brphen), 5-methyl-1,10-phenanthroline (5-Mephen), 4,7-Me_2phen, 5,6-dimethyl-1,10-phenanthroline (5,6-Me_2phen), 4,7-diphenyl-1,10-phenanthroline (4,7-Ph_2phen) and 3,4,7,8-tetramethyl-1,10-phenanthroline (3,4,7,8-Me_4phen). For all complexes, except where NN = 5-Phphen, 4,4′-Ph_2bpy and $Cr(trpy)_2^{3+}$, a slow emission rise is observed at 665 nm and above. Under similar experimental conditions, several luminescent systems exhibited neither slow "grow-in" of luminescence nor a fast emission component; these systems include $Ru(bpy)_3^{2+}-H_2O$, *trans*-$Cr(NH_3)_2(NCS)_4^- - H_2O$, *trans*-$Cr(en)_2(NCS)_2^+ - H_2O$, $Cr(en)_2F_2^+ - H_2O$, $Cr(en)_3^{3+} - H_2O$, eosineY–H_2O, biacetyl–methanol and biacetyl–heptane. The $Fe(bpy)_3^{2+} - H_2O$ system shows a biphasic emission decay, with a fast component ($\tau \approx 0.2$ ns) and a weak slower component ($\tau \approx 5$ ns). Furthermore, for the $Cr(5,6\text{-}Me_2phen)_3^{3+}$ system in the presence of sufficient iodide ion, I^-, to quench about 99% of the $^2T_1/^2E$ emission, the slow rise in luminescence is completely quenched while the fast emission component is slightly quenched. Also, 532 nm excitation of $Cr(5,6\text{-}Me_2phen)_3^{3+}$ (1×10^{-2} M) affords neither fast emission nor slow emission grow-in [71].

With the type of laser system utilized, and considering the constraints placed by weakly luminescent ($\phi_{lum} \leqslant 10^{-3}$) complexes and absorbance change values (ΔA) of 0.10–0.20 for excited state absorption, Serpone and Hoffman [71] have acknowledged the presence of multiphotonic effects in their earlier work [66]. Nonetheless, they did observe [71] the photophysics of chromium(III) complexes other than $Cr(NN)_3^{3+}$ not different from those of Rojas et al. [26,31,70]. Thus, for 355 nm laser excitation of $Cr(NN)_3^{3+}$, instrumental artifacts were clearly not responsible for the excited state behavior observed.

The luminescence features observed for $Cr(4,7\text{-}Me_2phen)_3^{3+}$ [66] and those of other chromium(III) polypyridyls, particularly of $Cr(5,6\text{-}Me_2phen)_3^{3+}$ [71] (Figs. 8–10), are better described by a model that involves two intermediates A and B that are precursors to the formation of $^2T_1/^2E$ states (intermediate C). Indeed, the slow emission grow-in observed for many of the $Cr(NN)_3^{3+}$ species examined could be fitted to the model for two consecutive first-order reactions [72] (eqns. (6) and (7)):

$$A \xrightarrow{k_1} B \xrightarrow{k_2} C \tag{6}$$

$$\gamma = 1 + [1/(1-k')]\left(k' e^{-\theta} - e^{-k'\theta}\right) \tag{7}$$

where k_1 and k_2 are the first-order rate constants, $\gamma = [C]/[A_0]$, $\theta = k_1 t$,

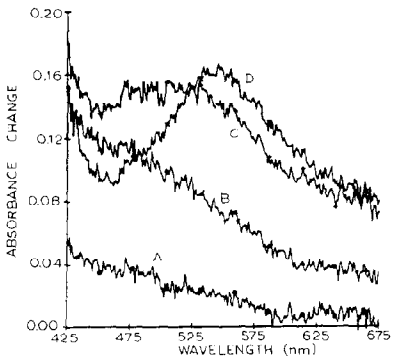

Fig. 11. Transient absorption spectra at − 50 ps (A), − 20 ps (B), 0 ps (C), and at + 50 ps (D) delay times from 355 nm laser excitation of $Cr(5,6\text{-}Me_2phen)_3^{3+}$ (from ref. 71).

$k' = k_2/k_1$, and $\alpha = e^{-\theta} = [A]/[A_0]$. In plots of γ vs. $(1 - \alpha)$ (from eqn. (6)) for $Cr(5,6\text{-}Me_2phen)_3^{3+}$, a best fit is obtained for $k' = 0.05$ with $k_1 \approx 2 \times 10^9$ s^{-1} and $k_2 \approx 1 \times 10^8$ s^{-1}. Intermediate A in eqn. (6) is identified with a transient whose $\tau \approx 0.5$ ns, and intermediate B with a transient whose $\tau \approx 10$ ns; B is the other precursor to the $^2T_1/^2E$ state (intermediate C in eqn. (6)). The intermediate species A and B have been identified [71] with the ^{1}LC and ^{3}LC coordinated ligand intraligand states respectively. A transient D with a decay time of about 50 ps is correlated with the lowest energy unrelaxed metal-centered $^4T_2$ state. Thus in the last model proposed, it appears that the events occurring in $Cr(NN)_3^{3+}$ complexes under the specified experimental conditions are caused by sequential, two monophotonic processes, whereby a discrete ground state species absorbs a photon, relaxes to a state with a lifetime of the same magnitude as the laser pulse duration, and subsequently absorbs an additional photon. A partitioning of energy from the ^{1,4}CTTS manifold(s) occurs between the upper quartet metal-centered (MC) states and the uppermost LC singlet states. The MC states cascade to the $^4T_2$ manifold while the LC states relax to the lowest ^{1}LC and ^{3}LC states. Transient absorption spectra (Fig. 11) and the related kinetics (Fig. 12) support the conclusions from transient emission. The $^2T_1$ and ^2E doublet states are thought to be populated primarily from the ligand-centered states (see Fig. 13) owing to the congruence of τ values of transient luminescence at 460 nm with those obtained from the fit to the slow "grow-in" of the $^2T_1/^2E$ luminescence; intersystem crossing occurs from ^{3}LC to ^{2}MC. Population of the $^2T_1/^2E$ manifold via the $^4T_2$ state does not appear significant, though undoubtedly it occurs, relative to other pathways. Evidently the importance of low lying LC states in these complexes cannot be ignored [71].

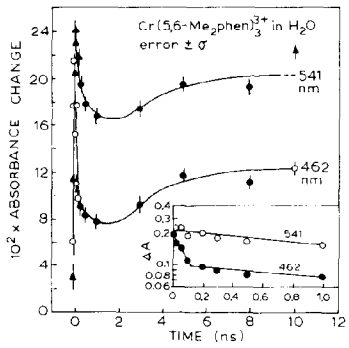

Fig. 12. Absorbance change vs. time at two wavelengths from the 355 nm excitation of $Cr(5,6\text{-}Me_2phen)_3^{3+}$. The inset is the semilogarithmic plot of ΔA vs. time. From ref. 71.

Also, the results reported by Serpone and Hoffman [71] and Rojas and Magde [70] are not inconsistent with each other, though they differ.

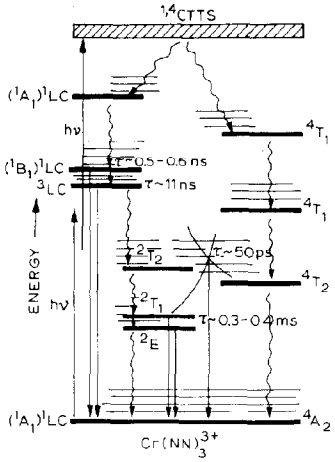

Fig. 13. Energy level diagram showing the relaxation pathways for the photophysical events arising from multiphoton excitation of $Cr(NN)_3^{3+}$ complexes. The lifetimes shown are for $Cr(5,6\text{-}Me_2phen)_3^{3+}$. From ref. 71.

(c) Iron(II), ruthenium(II), osmium(II)

Sutin and coworkers [73] have carried out an extensive study of the photophysics of iron(II), ruthenium(II) and osmium(II) polypyridine complexes, $M(NN)_3^{2+}$ or $M(trpy)_2^{2+}$, using a mode-locked Nd:glass laser. Quenching of the excited states of $Ru(NN)_3^{2+}$ and $Os(NN)_3^{2+}$ species by

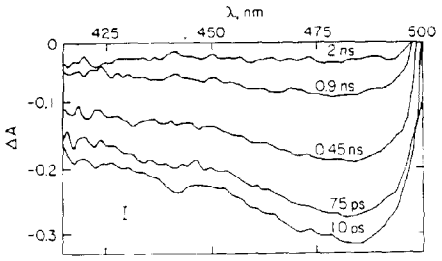

Fig. 14. Ground state bleaching of $Fe(phen)_3^{2+}$ at five different delay times after excitation with 527 nm light (from ref. 73).

ground state $M(NN)_3^{2+}$, and quenching of $Fe(bpy)_3^{2+}$ and $Fe(trpy)_2^{2+}$ by $Fe^{3+}(aq)$ ions have also been examined. Excitation of aqueous $Fe(NN)_3^{2+}$ and $Fe(trpy)_2^{2+}$ at ambient temperature with about 6 ps pulses of 527 nm light, results in bleaching of ground state absorption, followed by an exponential restoration of the ground state absorption (Fig. 14). $Os(NN)_3^{2+}$ complexes in aqueous media at 298 K were examined with a frequency-doubled Nd : YAG laser with 5 or 8 ns pulses of 530 nm light. The spectral properties and lifetimes for $M(NN)_3^{2+}$ and $M(trpy)_2^{2+}$ complexes are summarized in Table 6. In contrast with the 70 ps state found for $Fe(phen)_3^{2+}$ by Street et al. [74], Sutin proposes that the nanosecond state is formed quantitatively in < 10 ps for all $Fe(NN)_3^{2+}$ and $Fe(trpy)_2^{2+}$ complexes. The lifetime data in Table 6 show that the iron(II) complexes do not parallel the trends observed for the ruthenium(II) and osmium(II) complexes. This is consistent with a charge transfer (CT) excited state assignment for the osmium(II) and ruthenium(II) species, and an LF state ($^3T_1$ or $^5T_2$) for the iron(II) complexes. The relatively short ligand-insensitive lifetimes of the iron(II) complexes suggest perhaps that the radiationless decay of these complexes is different from that in osmium(II) and ruthenium(II) species, and that this difference may originate in substantially distorted excited state geometry for the iron(II) complexes. This investigation [74] and that of Kirk et al. [20] are in disagreement with that of Phillips et al. [76] who deduced a 33 ns lifetime for excited state $Fe(bpy)_3^{2+}$ by measuring photocurrents at an SnO_2 electrode with 459–514 nm excitation for the photooxidation of $Fe(bpy)_3^{2+}$ by $Fe^{3+}(aq)$. While the excitation wavelength ranges (459–514 nm for the electrochemical work vs. 530 nm for the laser) do not overlap, it is expected that the excited state obtained with 459–514 nm excitation would rapidly convert to the state achieved upon 530 nm excitation. One suspects that the observed photocurrents [76] are probably due to species adsorbed onto SnO_2 or due to some interfacial artifact.

TABLE 6

Spectral properties and lifetimes of $M(NN)_3^{2+}$ and $M(trpy)_2^{2+}$ (M = Fe, Ru, Os) complexes at 298 K [a]

Ligand	Fe		Ru		Os	
	τ (ns) in H_2O	Emission max. (nm)	τ (ns) in H_2O	Emission max. (nm)	τ (ns) in H_2O	Emission max. (nm)
trpy	2.54 ± 0.13	–	$\leqslant 5$	628	–	750
	–	–	$\geqslant 1.2$ [b]	–	–	–
bpy	0.81 ± 0.07	–	600	613, 627	19 ± 1	715
	0.83 ± 0.07 [c]		–	–	19 ± 2 [d]	–
4,4′-Me_2bpy	0.76 ± 0.04	–	330	–	9	735
4,4′-Ph_2bpy	–	–	–	–	52 ± 3 [e]	–
phen	0.80 ± 0.07	–	920	–	84	700
	0.71 ± 0.05	–	–	–	–	–
5,6-Me_2phen	–	–	1810	–	63	705
5-Mephen	–	–	1330	–	69	700
5-Clphen	–	–	940	605, 625	78	700
4,7-Ph_2phen	–	–	–	–	200 ± 20 [e]	–
4,7-$(SO_3Ph_2phen)^{2-}$	0.43 ± 0.03	–	3860	–	–	–

[a] Ref. 73, unless otherwise noted. [b] From R.C. Young, J.K. Nagle, T.J. Meyer and D.G. Whitten, J. Am. Chem. Soc., 100 (1978) 4773. [c] Ref. 20. [d] From C.-T. Lin and N. Sutin, J. Phys. Chem., 80 (1976) 97. [e] In ethanol at 298 K. [f] Ref. 75.

The excited state spectrum of $Fe(bpy)_3^{2+}$ (aqueous solution at ambient temperature) is featureless above ca. 300 nm; no absorption maxima are observed in the 270 510 nm region, though intense absorption is observed below 300 nm [73]. This contrasts with the excited state spectra of $Ru(bpy)_3^{2+}$ and $Os(bpy)_3^{2+}$, for which maxima are observed at ca. 360 nm and 430 nm for the ruthenium(II) complex and ca. 360 nm and 460 nm for the osmium(II) complex [73,77]. The spectral features of $^*Ru(bpy)_3^{2+}$ and $^*Os(bpy)_3^{2+}$ correlate with the LC transitions of a $(t_{2g})^5(\pi^*)^1$ MLCT excited state. Further, these spectra are similar and reminiscent of that of the 2,2′-bipyridyl radical anion [78]. The features of the excited state spectrum of $Fe(bpy)_3^{2+}$ suggest that $^*Fe(bpy)_3^{2+}$ does not possess the bipyridyl anion chromophore, and thus the excited state observed is not MLCT in nature. The nanosecond excited state attained upon 530 nm excitation [73] is an LF state, either $^3T_1$ $((t_{2g})^5(e_g)^1)$ or $^5T_2$ $((t_{2g})^4(e_g)^2)$, with an energy of about 0.9 eV above the ground state. An excited state reduction potential of $^*E^0_{3,2} \geqslant +0.1$ V for the $Fe(bpy)_3^{3+}/^*Fe(bpy)_3^{2+}$ couple follows from using an excitation energy of

0.9 eV or more and an $Fe(bpy)_3^{3+}/Fe(bpy)_3^{2+}$ reduction potential of 1.05 eV.

Evidence for the photoinduced oxidation of $Fe(bpy)_3^{2+}$ in a non-aqueous aluminum chloride–ethylpyridinium bromide melt has been cited by Chum et al. [75]. Upon irradiation with low intensity visible light ($\lambda > 400$ nm), most of the iron(II)–diimine complexes investigated are converted to iron(III) species. The ethylpyridinium cation, $Etpy^+$, is thought to be the electron accepting species. The similarities observed between this system and $Ru(bpy)_3^{2+}$ and the observation [79] that $*Ru(bpy)_3^{2+}$ is quenched by *para*-substituted alkylpyridinium ions suggest that $Etpy^+$ quenches the MLCT excited state in $Fe(bpy)_3^{2+}$.

The quenching mechanism of $*Fe(bpy)_3^{2+}$ is not well understood. It is likely that the excited state $*Fe(bpy)_3^{2+}$ undergoes photooxidation very slowly in water at 298 K [73], and that in the presence of large concentrations of highly reactive electron acceptor species (e.g. 3.2 M ethylpyridinium bromide) [75], photoinduced oxidation may occur more readily. A comparison of the iron(II), ruthenium(II) and osmium(II) polypyridine complexes shows that the excited states of $Fe(NN)_3^{2+}$ are much less reactive than those of the $Ru(NN)_3^{2+}$ and $Os(NN)_3^{2+}$ complexes because of their lower excitation energy and their electron configuration which afford a higher kinetic barrier to electron transfer.

Two distinct relaxation rates are observed upon 527 nm excitation (6 ps FWHM pulses) of $Fe(phen)_3^{2+}$ in an ethanol–methanol (4 : 1 v/v) mixture at low temperatures (14 and 81 K) [80]. At higher temperatures (140, 200 and 295 K), single-exponential decays are seen; the data are collected in Table 7. The former observation would seemingly imply the presence of two (or more) kinetically important excited states. The longer-lived excited states are likely to possess ligand-field character (^3LF, ^5LF) since the initially populated excited state is a ^1MLCT state while the excited state present

TABLE 7

Excited state decay rates for $Fe(phen)_3^{2+}$ in ethanol–methanol (4 : 1 v/v) mixtures at various temperatures [a]

T (K)	λ_1 (10^8 s^{-1})	τ_1 (ps)	λ_2 (10^8 s^{-1})	τ_2 (ns)
14 [b]	17 ± 3	580 ± 200	1.7 ± 0.4	6.0 ± 1.3
81 [b]	30 ± 5	340 ± 130	2.7 ± 0.4	3.7 ± 0.5
140 [c]			2.7 ± 0.4	3.7 ± 0.5
200 [c]			3.4 ± 0.3	2.9 ± 0.2
295 [c]			7.4 ± 0.7	1.4 ± 0.2

[a] Ref. 80. [b] Decays fit to a double exponential: $\Delta A(t) = A_0[(1-\beta)e^{-\lambda_1 t} + \beta e^{-\lambda_2 t}]$. [c] Decays fit to a single exponential: $\Delta A(t) = A_0 e^{-\lambda t}$.

10 ps after excitation has a molar absorptivity < 900 $M^{-1}\,cm^{-1}$ at 456 nm. $Fe(phen)_3^{2+}$ is expected to show strong absorption in the visible region inasmuch as the ^{3}MLCT excited states of $Ru(bpy)_3^{2+}$ and $Os(bpy)_3^{2+}$ do show strong visible absorption [73]. Further, at room temperature the excited state $^*Fe(bpy)_3^{2+}$ decays with a lifetime of less than 1 ns (Table 6), a complex for which an LF excited state assignment was made.

Because of the different nature of the excited states, ESA and circular dichroism (CD) spectra of (Δ)-$Fe(bpy)_3^{2+}$ may differ from those of (Δ)-$Ru(bpy)_3^{2+}$, which exhibits a small CD [81] in the bpy $\pi\pi^*$ transition at 370 nm, consistent with a single-ligand localized model for the transferred electron in the excited state. A large CD is observed in the $\pi\pi^*$ transitions of the excited (Δ)-$Fe(bpy)_3^{2+}$ species in water. Additionally, ESA assigned to ligand $\pi\pi^*$ is observed in the 280–305 nm region. The excited state CD spectrum is red shifted and somewhat diminished in intensity relative to the ground state CD spectrum. A comparison of ground and excited state spectra reveals a red shift and diminished intensity of the $\pi\pi^*$ transitions for the excited state species in both absorption and CD spectra. A red shift in the $\pi\pi^*$ absorption is envisioned since there are no observable visible CT states to interact with the $\pi\pi^*$ states, thereby affording a higher energy shift. Both the $^3T_1$ and $^5T_2$ states may play a vital role in the excited state kinetics and spectroscopy. A strong CD in the red-shifted $\pi\pi^*$ transitions is not unexpected in that the ligand-field nature of the metastable excited state(s) should not suppress exciton coupling among the three $\pi\pi^*$ transitions in the bpy ligands. The excited state absorption and CD spectra of $Fe(bpy)_3^{2+}$ in water are compatible with a d–d excited state portrait.

A method has been developed [82] to determine the quantum yields of non-luminescent excited states and photoproducts with subnanosecond lifetimes utilizing picosecond absorption spectroscopy (6 ps FWHM pulses, 527 nm excitation). Since optically thick samples ($A > 0.05$) are used to obtain significant change-in-absorbance (ΔA) values, the intensity of the photoexcitation pulse will vary as it propagates through the sample, as will the absorbance of the sample. Thus it becomes necessary to calculate the percentage excitation of a given sample as a function of the incident excitation flux.

The quantum yield (ϕ) of the lowest energy LF excited state of $Fe(phen)_3^{2+}$ has been determined to ascertain whether the higher-energy states (^{1,3}MLCT and $^3T_1$) populate the $^5T_2$ state with unit efficiency or whether they decay to the ground state. The technique affords $\phi = 1.00 \pm 0.05$, a value compatible with that reported for $Fe(bpy)_3^{2+}$ ($\phi = 1.6 \pm 0.5$), using nanosecond laser spectroscopy [73].

Figure 15 depicts a kinetic model for $Fe(NN)_3^{2+}$ as it has evolved. To summarize, the strong visible absorption bands represent MLCT transitions.

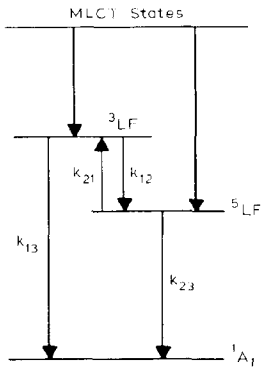

Fig. 15. Kinetic scheme for MLCT state population of lower energy LF states in iron(II) polypyridine complexes: the ^{5}LF is the $^5T_2$ state and the ^{3}LF state is $^3T_1$. From ref. 82.

The MLCT states are rather short lived ($\tau < 10$ ps), and thus only the subsequently populated LF states ($^3T_1$, $^5T_2$) are observed. It is assumed that the initially formed MLCT states exclusively populate the $^3T_1$ state, though one cannot exclude the possibility that the MLCT states directly populate the $^5T_2$ state. However, the ^{1,3}MLCT and $^3T_1$ states do not directly populate the $^1A_1$ ground state [82].

Picosecond Raman spectroscopy (30, 80 and 150 ps pulses) studies of $Ru(bpy)_3^{2+}$ in water and in glycerol at 295 K have been carried out to ascertain whether, upon photoinduced metal-to-ligand charge transfer, the electron is initially localized on a single bpy ligand or delocalized over the three-bpy ligand system [83]. Whereas in room temperature media it is suggested [84–87] that localization is complete in a nanosecond or picosecond timeframe, evidence from solid state and low temperature glass investigations suggests an initially delocalized electron evolving toward a localized configuration [88–90].

The picosecond Raman spectrum of $Ru(bpy)_3^{2+}$ in water at 295 K (Fig. 16) corresponds to that of the excited state wherein the electron is localized on a single bpy ligand with charge localization complete in less than 30 ps. In glycerol at 295 K, however, the intensity of the Raman bands associated with localized MLCT states is diminished relative to that in water for a 150 ps excitation pulse. The band intensities further decrease in glycerol for a 30 ps pulse, implying some dynamic dependence of the excited state bands in glycerol, as this effect is not observed in water. Chang et al. [83] attribute these observations to an initially delocalized electron. Electron trapping follows as solvation transpires, giving rise to a localized electron configuration.

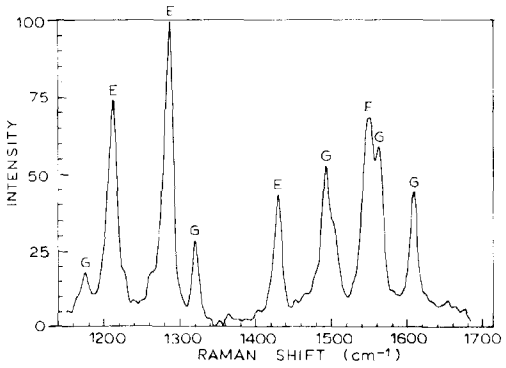

Fig. 16. Picosecond resonance Raman spectrum of $Ru(bpy)_3^{2+}$ in water; the letters E, G and S denote the Raman bands for the excited state of $Ru(bpy)_3^{2+}$, the ground state of $Ru(bpy)_3^{2+}$, and the solvent respectively (from ref. 83).

(d) Iron(III), osmium(III)

The ligand-to-metal charge transfer (LMCT) excited states of iron(III) and osmium(III) polypyridine complexes are expected to be very short lived since detectable luminescence is not observed at ambient temperatures. It is plausible that low energy LF states may be responsible for the short lifetimes of the iron(III) complexes; however, the LF states in the osmium(III) complexes would appear too high in energy to be populated in the LMCT transition. Picosecond absorption spectroscopy (6 ps pulses, 527 nm excitation) has been employed to determine the LMCT excited state lifetimes of $Fe(phen)_3^{3+}$, $Fe(bpy)_3^{3+}$, $Os(phen)_3^{3+}$ and $Os(bpy)_3^{3+}$ as a function of isotopic composition as well as temperature [91].

The increases in ΔA in the 420–460 nm region of $Fe(phen)_3^{3+}$ and $Os(phen)_3^{3+}$ following 527 nm excitation are consistent with an LMCT excited state assignment. The lifetimes are collected in Table 8 along with pertinent data for the corresponding iron(II) and osmium(II) complexes. It should be noted that for $Fe(phen)_3^{3+}$ and $Os(phen)_3^{3+}$ ($\tau = 2$–9 ps) at 295 K, the temporally symmetric ΔA signals observed indicate that the lifetimes of the initially populated LMCT states are shorter than the photolysis pulse of 6 ps (see Fig. 17). Thus the lifetime of 2–9 ps represents excited states observable during but not subsequent to excitation, and they are not unobservable excited states ($\tau < 2$ ps) [91].

There is no evidence for long-lived LF states in $Fe(phen)_3^{3+}$, as found [80] for $Fe(phen)_3^{2+}$. This is attributed [91] to the relative energies of LF and CT states in the iron(II) and iron(III) complexes. The rapid deactivation of the

TABLE 8

Charge-transfer excited state lifetimes of iron(III) and osmium(III) polypyridine complexes [a]

Complex	Lifetime (ps)	Temperature (K)
$Fe(phen)_3^{3+}$	2–9 [b]	295
	14 ± 3 [b]	80
	12 ± 3 [b]	10
$Fe(phen)_3^{2+}$	$\leqslant 10$ [c]	295
	$\leqslant 10$ [c]	14
$Os(phen)_3^{3+}$	2–9 [b]	295
	20 ± 3 [b]	80
	19 ± 2 [b]	10
$Os(bpy)_3^{3+}$	62 ± 4 [a]	5
	64 ± 4 [d]	5
$Os(bpy\text{-}d_8)_3^{3+}$	120 ± 10 [e]	10
$Os(phen)_3^{2+}$	32.2 μs [f]	4
$Os(bpy)_3^{2+}$	1.05 ± 0.04 μs [e]	10
	10.8 μs [f]	4.2
$Os(bpy\text{-}d_8)_3^{2+}$	2.5 ± 0.2 μs [e]	10

[a] Ref. 91. [b] In 9 M H_2SO_4–H_2O. [c] Ref. 80. [d] In 9 M D_2SO_4–H_2O. [e] In 9 M D_2SO_4–D_2O. [f] From D. Lacky, B.J. Pankuch and G.A. Crosby, J. Phys. Chem., 84 (1980) 2068.

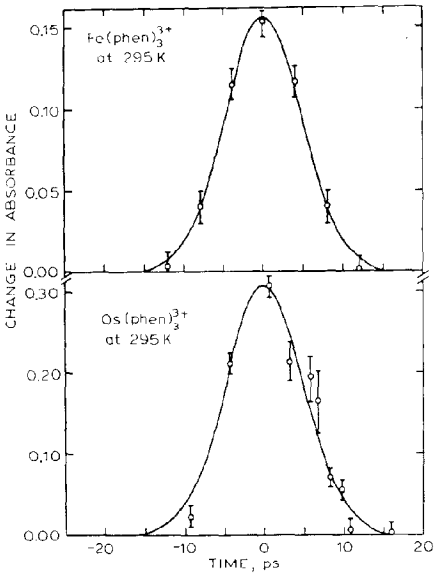

Fig. 17. Change in absorbance vs. probe pulse arrival time relative to the excitation pulse monitored at 460 nm ($Fe(phen)_3^{3+}$) and at 470 nm ($Os(phen)_3^{3+}$). The FWHM is 11 ps. From ref. 91.

initially populated MLCT $(Fe(phen)_3^{2+}$ and LMCT $(Fe(phen)_3^{3+}$ excited states is provided by low lying LF excited states. The absence of any low lying excited states in $Os(NN)_3^{2+}$ is compatible with the relatively long lifetimes of these excited state complexes. The dominant reason for the short lifetimes of $(LMCT)Os(NN)_3^{3+}$ is reported [91] to be the smaller energy gaps present in these complexes compared with those in the corresponding osmium(II) complex. It appears that the observed mid-frequency (1300–1600 cm^{-1}) skeletal stretching vibrations (C–C, C–N) of the polypyridine ligands are very important in the active modes of non-radiative decay of $(CT)Os(NN)_3^{2+/3+}$ complexes [91].

(e) Rhodium(III)

The risetimes of the luminescence (350–630 ns) from *cis*-$[RhX_2(bpy)_2]X$ (X = Cl, Br) have been measured in solution at room temperature and 77 K. Emission decay times in solution at room temperature (and 77 K) are 11.6 μs (45.2 μs) for $[RhCl_2(bpy)_2]Cl$ and 2.4 μs (26.5 and 3.6 μs) for $[RhBr_2(bpy)_2]Br$. It was later realized that the risetimes were actually the time constants of the detection system used, and not the intrinsic risetimes [92]. Time-resolved (10 ns pulses, 306 nm excitation) transient absorption spectra of *cis*-$[RhCl_2(bpy)_2]Cl$ and *cis*-$[RhBr_2(bpy)_2]Br$ (Fig. 18) in air-equilibrated ethanol–methanol (4 : 1 v/v) solution at room temperature reveal transients with lifetimes of 84 ns and 54 ns respectively; in de-oxygenated solutions, the lifetimes are significantly longer. The transient spectra are assigned [93] to $T_1 \rightarrow T_n$ transitions (see Fig. 19). ESA spectra obtained via excitation of $[RhX_2(bpy)_2]X$ with a 306 nm subpicosecond

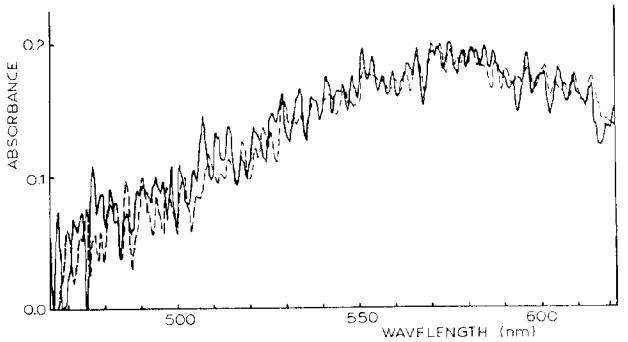

Fig. 18. Picosecond time-resolved absorption spectra of $[RhBr_2(bpy)_2]Br$ after 1 ps (solid curve) and 17 ps (broken curve) on excitation with subpicosecond pulses at 306 nm (from ref. 93).

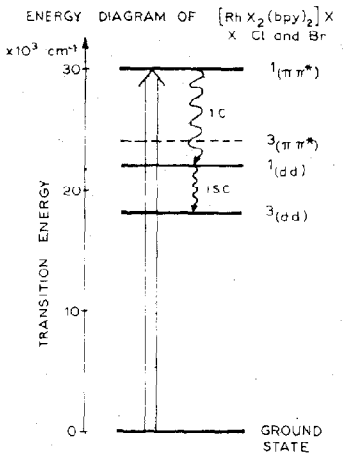

Fig. 19. Energy level diagram for $[RhX_2(bpy)_2]X$ (from ref. 93).

pulse correspond to the $T_1 \rightarrow T_n$ absorption spectra observed by nanosecond spectroscopy. The risetime for the transient absorbance change is equal to about 2.4 ps for X = Cl and about 1.3 ps for X = Br.

For $[RhX_2(bpy)_2]X$ complexes, excitation in the 306–347.2 nm region is to an LC $^1(\pi\pi^*)$ configuration, while the phosphorescent state (the lowest triplet state) is of localized $^3(dd)$ configuration. Hence, the relaxation processes from the initially populated $^1(\pi\pi^*)$ state and emission involve changes in orbital parentage (internal conversion (ic)) and spin multiplicity (isc). The "effective" relaxation rate to the phosphorescent $^3(dd)$ state is estimated at about 4×10^{11} s^{-1} for X = Cl and about 8×10^{11} s^{-1} for X = Br. Relaxation probably occurs from $^1(\pi\pi^*)$ to $^1(dd)$ via internal conversion and intersystem crossing to $^3(dd)$. Thus the "effective" relaxation rates correspond to the rates of $^1(dd) \rightarrow {}^3(dd)$ intersystem crossing.

(f) Iridium(III)

Picosecond time-resolved absorption spectra (0.5 ps pulses, 306 nm excitation) of *cis*-$[IrCl_2(phen)_2]^+$ in ethanol–methanol (4 : 1 v/v) at 2, 7, 12, 54 and 75 ps after the excitation pulse (Fig. 20) have been used to determine the formation time of the lowest triplet excited state, T_1; $\tau = 26 \pm 10$ ps in good agreement with the decay time of the species "P" (see below). The spectrum obtained by nanosecond spectroscopy arises [93] from $T_1 \rightarrow T_n$ absorption inasmuch as the T_1 lifetime of this complex is 60 ns at 292 K in degassed solution, and equal to the phosphorescence lifetime. The corre-

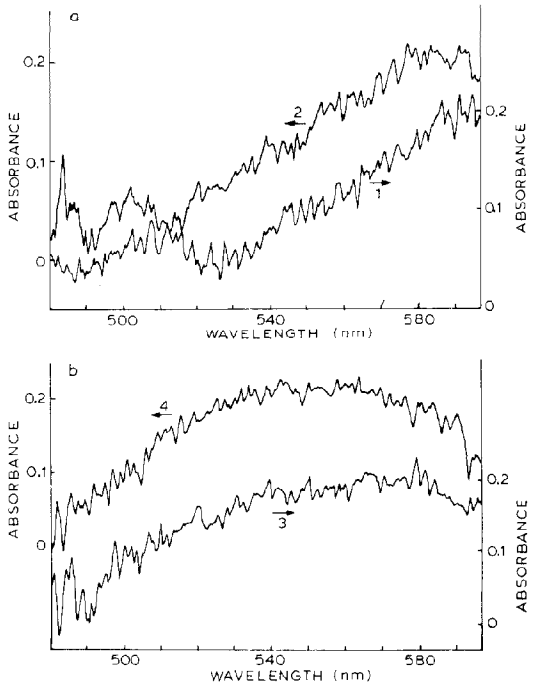

Fig. 20. Picosecond time-resolved absorption spectra of *cis*-$IrCl_2(phen)_2^+$ in an ethanol–methanol mixture: curve 1, at 2 ps after subpicosecond 306 nm laser excitation; curve 2, at 7 ps; curve 3, at 54 ps; curve 4, at 75 ps (from ref. 93).

spondence between the decay time of species "P" and the risetime of T_1 implies that "P" is a precursor of T_1.

Ohashi and Kobayashi have determined the $T_1 \rightarrow T_n$ absorption spectra [94] and time constants for the formation of the lowest triplet state, T_1 [95] for *cis*-$[IrCl_2(phen)_2]Cl$ in DMF–H_2O (95% v/v and 45% v/v) mixtures and in pure H_2O using a nitrogen laser and a mode-locked ruby laser (20 ps pulses, 347.2 nm excitation). The time constant for intersystem crossing $S_1 \rightarrow T_1$ (S_1 is the lowest excited singlet state) is 37 ps in DMF–H_2O (45% v/v) and 26 ps in DMF–H_2O (95% v/v), and is interpreted in terms of a change in the character of the T_1 state along with a change in solvent polarity. Hence, in an ethanol–methanol (4 : 1 v/v) medium, a time constant of 26 ps for T_1 formation is in accord with this notion, and is attributed to intersystem crossing from S_1 to T_1 with the species "P" assigned to S_1 [93]. The lowest excited singlet state S_1 corresponds to a $d\pi^*$ state, and the lowest $^3(d\pi^*)$ and $^3(\pi\pi^*)$ states lie just below S_1 in water, as determined

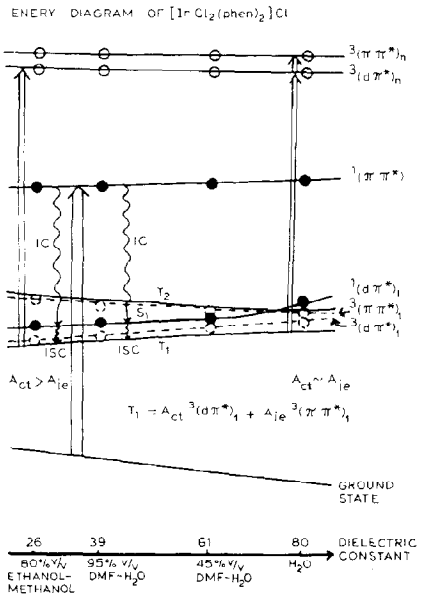

Fig. 21. Energy level diagram for $IrCl_2(phen)_2^+$ (from ref. 93).

from ground state absorption spectroscopy. Thus the $S_1 \rightarrow T_1$ process involves either $^1(d\pi^*) \rightarrow {}^3(d\pi^*)$ or $^1(d\pi^*) \rightarrow {}^3(\pi\pi^*)$. In DMF H_2O (95% v/v), T_1 is a $^3(d\pi^*)$ state; but with an increase in solvent polarity, the $^3(d\pi^*)$ state shifts to higher energy and mixes with $^3(\pi\pi^*)$. In this solvent system, the S_1 state is situated between $^3(d\pi^*)$ and $^3(\pi\pi^*)$ and shifts to a higher energy with increasing solvent polarity (Fig. 21).

(g) Copper(I)

Copper(I) polypyridine complexes possess low lying MLCT excited states [96,97]. Photoinduced electron transfer occurs from $Cu(2,9\text{-}Me_2phen)_2^+$ (2,9-Me_2phen = 2,9-dimethyl-1,10-phenanthroline) to various cobalt(III) complexes in solution [98]. Furthermore, $Cu(2,9\text{-}Me_2phen)_2^+$ is luminescent ($\tau = 54$ ns in CH_2Cl_2 at ambient temperature) in weak donor solvents [99], though a prior study [100] reports the complex to be non-emissive in methanol. The complex does luminesce in the solid state [101], though apparently not in acetone, CH_3CN or H_2O in which the luminescence efficiency is estimated [99] to be very small.

Emission quenching of copper(I) species in the presence of Lewis bases (e.g. CH_3CN, MeOH) is thought [102] to occur via exciplex formation (i.e.

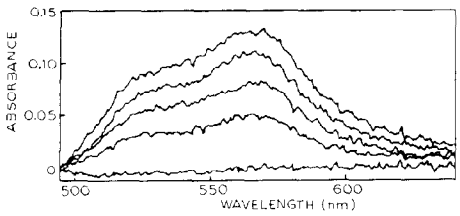

Fig. 22. Time-resolved absorbance difference spectra of $Cu(2,9\text{-}Me_2phen)_2^+$ in CH_3CN at 20 °C. From top to bottom, the delay times are 47 ps, 347 ps, 1.01 ns, 1.68 ns and 8.35 ns following the excitation pulse. From ref. 105.

excited state complex formation). Moreover, related copper(II) complexes are pentacoordinate [103,104], consistent with an associative quenching process in which the coordination number of the copper center increases from four to five since the metal center is formally divalent in the CT excited state (square planar).

Picosecond excited state absorption and temperature dependence studies have been carried out [105] for $Cu(2,9\text{-}Me_2phen)_2^+$ and $Cu(2,9\text{-}Me_2\text{-}4,7\text{-}Ph_2phen)_2^+$ (2,9-Me_2-4,7-Ph_2phen = 2,9-dimethyl-4,7-diphenyl-1,10-phenanthroline) in various Lewis bases (CH_3CN, acetone, *p*-dioxane) to elucidate further the excited state behavior of this type of complex. ESA spectra (30 ps pulses, 355 nm excitation) of $*Cu(2,9\text{-}Me_2phen)_2^+$ and $*Cu(2,9\text{-}Me_2\text{-}4,7\text{-}Ph_2phen)_2^+$ in CH_2Cl_2 reveal maxima at 570 nm and 610 nm respectively. The time-resolved absorbance difference spectrum exhibits GSB at $\leqslant 520$ nm for the 2,9-Me_2-4,7-Ph_2phen complex. For the analogous 2,9-Me_2phen complex the spectrum is similar in both CH_2Cl_2 and CH_3CN, though in CH_3CN the absorbance difference spectrum (Fig. 22) decays with a time constant of 2.0 ± 0.3 ns; its emission lifetime is 55 ns in CH_2Cl_2. The spectra are characteristic of their respective ligand radical anions, and thus a CT excited state assignment is plausible for $Cu(2,9\text{-}Me_2phen)_2^+$ in CH_3CN ($\tau = 2.0 \pm 0.3$ ns at 293 K) [105].

A kinetic study (luminescence lifetime method) of the quenching of $*Cu(2,9\text{-}Me_2phen)_2^+$ in CH_3CN, acetone and *p*-dioxane in CH_2Cl_2 solution shows that quenching implies the formation of an exciplex, $*Cu \cdots Q$, followed by deactivation (eqns. (8)–(10)):

$$*Cu(CT) \rightarrow Cu(k_0 = 1/\tau_0) \tag{8}$$

$$*Cu + Q \underset{k_{-1}}{\overset{k_1}{\rightleftharpoons}} *Cu \cdots Q \tag{9}$$

$$*Cu \cdots Q \xrightarrow{k_q} Cu + Q \tag{10}$$

However, no accumulation of the exciplex $*Cu \cdots Q$ is observed experimentally probably owing to extremely fast radiationless decay processes involving the exciplex. Temperature dependence studies give $\Delta H^{\neq} = -12$ kJ mol^{-1}, $\Delta S^{\neq} = -150$ J mol^{-1} K^{-1} (acetone) and $\Delta H^{\neq} = -2$ kJ mol^{-1}, $\Delta S^{\neq} = -110$ J mol^{-1} K^{-1} (CH_3CN). The very negative $\Delta S^{\neq}$ values explain the observed decrease in k_q values with increasing temperature. The exciplex $*Cu \cdots Q$ is thought to be a species in which the quencher Q (Lewis base) acts as a fifth donor for the copper center (eqn. (11)) [105]. Taking this view, there should be no barrier to exciplex formation; however, an activation requirement can develop from some other process such as desolvation and structural reorganization.

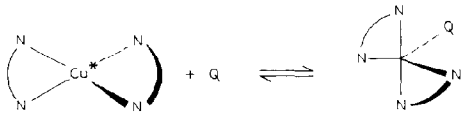

E. SPECTROSCOPY OF BINUCLEAR METAL COMPLEXES

An interesting chapter in the study of binuclear complexes concerns the pairing of two d^4 transition metal ions in molecules having metal–metal bonds in their ground states. Specifically, it is of interest to ascertain and identify the excited state(s) reached upon picosecond laser excitation, the geometry, and the lifetime of this (these) excited state(s).

Molecular orbital (MO) theory predicts that, for a d^4–$d^4M_2X_8^{n-}$ complex of D_{4h} symmetry, eight d electrons from the two metal ions fill four metal–metal bonding orbitals yielding a $\sigma^2\pi^4\delta^2$ ground state configuration and a quadruple bond. The theory correctly predicts a diamagnetic ground state and an eclipsed (D_{4h}) ligand conformation. Additionally, MO theory predicts a dipole- and spin-allowed $\delta^2 \rightarrow {}^1(\delta\delta^*)$ excitation present in absorption spectra. Several groups [106–113] have observed visible absorption bands (500–700 nm) assigned to the ${}^1A_{1g} \rightarrow {}^1A_{2u}$ transition. The bands are polarized parallel to the M M bond, while at low temperatures they resolve into vibrational progressions in the M–M stretching mode. Such progressions suggest an increase in the M–M distance as a consequence of there being no δ bond in the ${}^1(\delta\delta^*)$ excited state. A staggered conformation for the ${}^1(\delta\delta^*)$ excited state is thought [112,114] to be more stable as a result of the M–M separation with no accompanying steric hindrances. Hay [114] has done ab initio calculations (valence bond (VB) theory) of the electronic structure of $Re_2Cl_8^{2-}$. In the VB theory, the ${}^1A_{1g}$ ground state has one electron in each d_{xy} orbital. At a slightly higher energy, the ${}^3A_{2u}$ excited

state has one electron in each d_{xy} orbital, but now triplet paired and corresponding to the $^3(\delta\delta^*)$ excited state predicted by MO theory. Two ionic singlet excited states arise from antisymmetric ($^1A_{2u}$) and symmetric ($^1A_{1g}$) combinations with both d_{xy} electrons on one metal center. A large $^1A_{2u} \rightarrow {}^3A_{2u}$ energy gap is predicted [115] by VB theory, and calculated [114] for $Re_2Cl_8^{2-}$. The only spin- and dipole-allowed transition here is the $^1A_{1g} \rightarrow {}^1A_{2u}$, corresponding to a metal-to-metal charge-transfer (MMCT) transition that correlates with the $\delta^2 \rightarrow {}^1(\delta\delta^*)$ transition from MO theory.

The lowest energy absorption band in the electronic spectra of $M_2X_8^{n-}$ complexes has been assigned to the $^1A_{1g} \rightarrow {}^1A_{2u}$ (MMCT) transition, though Mathisen et al. [116] and Stromberg [117] have questioned this assignment. However, there is indecision as to the assignment of the luminescence band maximizing just to the red of the $^1A_{1g} \rightarrow {}^1A_{2u}$ absorption band. For $Mo_2Cl_8^{4-}$, $Re_2Cl_8^{2}$ and $Re_2Cl_8^{2-}$, mirror-image absorption and emission spectra do not prevail [112,118], and their apparent band origins do not overlap [108]. In contrast, mirror-image absorption and emission spectra have been obtained for $Mo_2X_4(PR_3)_4$ complexes (X = Cl, Br, I; R = alkyl) [112,119,120].

In an effort to delineate the lack of mirror-image absorption and emission spectra in $M_2X_8^{n}$ -type complexes, Winkler et al. [121] have investigated the transient absorption spectra of $Mo_2Cl_8^{4-}$, $Re_2Cl_8^{2-}$, $MoCl_4(CH_3CN)_4$ and $Mo_2Cl_4(PBu_3)_4$. Fraser and Peacock [118] suggest that the luminescence from $K_4[Mo_2Cl_8]$ in a pressed KCl disc at about 10 K involves states with substantial Mo–Cl bonding or antibonding character, i.e. the ^3E_g or $^3A_{2g}$ state. The picosecond transient absorption kinetic study [121] of $Mo_2Cl_8^{4-}$, $Re_2Cl_8^{2-}$, $MoCl_4(CH_3CN)_4$ and $Mo_2Cl_4(PBu_3)_4$ reveals the following. $Re_2Cl_8^{2-}$ in CH_3CN features an absorption maximum at 682 nm ($\delta^2 \rightarrow {}^1(\delta\delta^*)$) and a broad emission centered around 780 nm [112]. The observed transient absorption maximum (390 nm) decays with the same lifetime as the luminescence (140 ns) [122]. Thus the luminescence arises from the $^1(\delta\delta^*)$ excited state in which the complex has a staggered D_{4d} geometry, and the transient absorption at 390 nm is an LMCT transition. Picosecond laser excitation at 650 nm shows a long-lived excited state formed in less than 20 ps. Assuming that previous assignments are correct, this transient arises from the $^1(\delta\delta^*)$ excited state, and rotation about the Re–Re axis that affords this state occurs within 20 ps.

$Mo_2Cl_8^{4-}$ in CH_3CN features a broad absorption maximum around 515 nm, and an emission maximum blue-shifted beyond observation [122]. However, upon picosecond laser excitation an excited state forms within 20 ps with a lifetime of 205 ps [121]. If indeed these $^1(\delta\delta^*)$ excited states prefer a staggered geometry, then the eclipsed-to-staggered conformational change is accomplished within 20 ps of excitation.

In $Mo_2Cl_4(CH_3CN)_4$, the absorption maximum is observed at 600 nm in

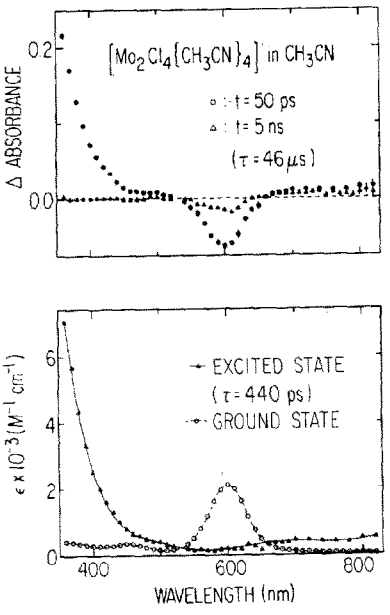

Fig. 23. Transient difference spectra (top) and ground and excited state absorption spectra (bottom) for $Mo_2Cl_4(CH_3CN)_4$ in CH_3CN recorded with 532 nm laser excitation. Delay times are indicated. From ref. 121.

CH_3CN. One $^1(\delta\delta^*)$ MMCT excited state is formed in less than 20 ps, as observed by transient absorption spectroscopy (Fig. 23). This suggests that $Re_2Cl_8^{2-}$, $Mo_2Cl_8^{4-}$ and $Mo_2Cl_4(CH_3CN)_4$ all demonstrate only staggered, and not eclipsed, $^1(\delta\delta^*)$ excited states. A kinetic investigation of the transient difference spectra of $Mo_2Cl_4(CH_3CN)_4$ recorded 50 ps and 5 ns after excitation shows two transient species with lifetimes of 440 ps and 46 μs. The first transient exhibits a strong absorption at $\lambda \leqslant 370$ nm, with $\epsilon_{max} > 7000\ M^{-1}\ cm^{-1}$, and probably arises from LMCT transitions of the $^1(\delta\delta^*)$ excited state. The long-lived (46 μs) transient species is thought [122] to be a structurally distorted derivative of $Mo_2Cl_4(CH_3CN)_4$ on the basis of structural and spectral consistencies.

The $Mo_2Cl_4(PBu_3)_4$ complex has been investigated in CH_2Cl_2 and CH_3CN [121]. In CH_2Cl_2, the luminescence decay time is 9.0 ± 0.4 ns. Transient difference spectra, however, reveal two transient decay times, 9 ns and 90 ns (Fig. 24). The 9 ns transient corresponds to the eclipsed $^1(\delta\delta^*)$ excited state in so far as the luminescence spectrum of the complex is the mirror image of the $\delta^2 \rightarrow {}^1(\delta\delta^*)$ absorption profile, and the luminescence

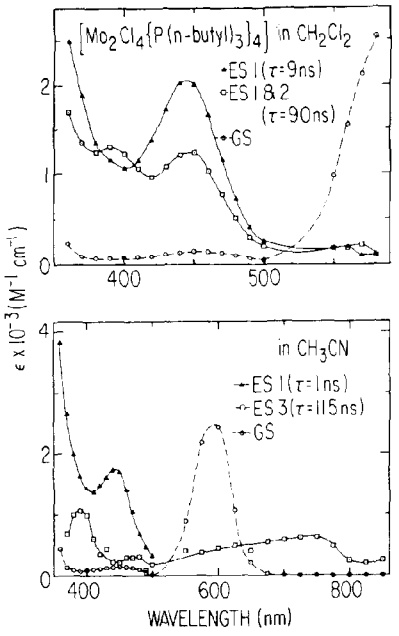

Fig. 24. Ground and excited state spectra of $Mo_2Cl_4(PBu_3)_4$ in CH_2Cl_2 (top) and CH_3CN (bottom) (from ref. 121).

lifetime is 9 ns. A reliable assignment of the excited state corresponding to the long-lived (90 ns) transient species is elusive at present, though the $^3(\delta\delta^*)$ state, the $^3(\pi\delta^*)$ excited state and a distorted chemical intermediate must all be considered. Transient difference spectra of $Mo_2Cl_4(PBu_3)_4$ in CH_2Cl_2 have been recorded at 230 ps and 11.5 ns after 532 nm laser excitation. The 230 ps spectrum, associated with the $^1(\delta\delta^*)$ state, shows an absorption maximum at 440 nm as well as absorption in the near-UV region ($\lambda < 400$ nm). The near-UV absorption probably arises from CT transitions; the absorption at 440 nm is ascribed to CT transitions involving phosphine ligands or a metal-localized excitation, $^1A_{2u}(\delta\delta^*) \rightarrow {}^1E_g(d\pi^*)$. In the 11.5 ns spectrum, where the $^1(\delta\delta^*)$ excited state is now 70% relaxed, there appears absorption at ca. 390 nm. This absorption, not observed in the $^1(\delta\delta^*)$ spectrum, suggests the presence of a different transient species whose identity could not be established in CH_2Cl_2 owing to overlapping absorptions. In CH_3CN, $Mo_2Cl_4(PBu_3)_4$ exhibits a luminescence decay time of 4.0 ± 0.3 ns; three relaxation processes ($\tau = 1$, 4 and 115 ns) are obtained by transient absorption kinetics at 580 nm [121]. Transient difference spectra for the complex in CH_3CN (Fig. 25) suggest that the 1 ns decay of the first

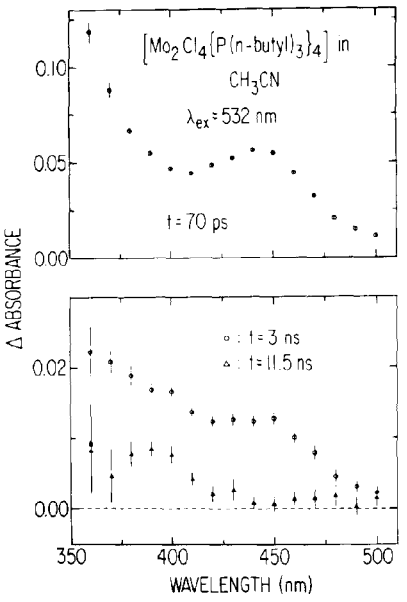

Fig. 25. Transient difference spectra for $Mo_2Cl_4(PBu_3)_4$ in CH_3CN recorded 70 ps (○, upper), 3 ns (○, lower) and 11.5 ns (▲, lower) after 532 nm laser excitation (from ref. 121).

transient to the second transient correlates with $^1(\delta\delta^*)$ nuclear relaxation while spectra, ab initio calculations and steric requirements argue for a distorted intermediate species to be associated with the long-lived (115 ns) transient. A conclusive assignment of the latter transient must await further study. What is interesting, though, is that this transient does not luminesce upon 532 nm laser excitation, in contrast with the long-lived transient species produced in CH_2Cl_2 [121].

Investigations of the d^8–d^8 binuclear complexes, analogous to those of the d^4–d^4 complexes, in terms of MO and VB theories have shown that the lowest energy singlet and triplet excited states of the d^8–d^8 complexes possess a $(d\sigma^* p\sigma)$ electronic configuration [123–127]. This configuration evolves to $^{1,3}A_{2u}$ excited states in tetragonal (local D_{4h} symmetry) complexes such as $Rh_2(TMB)_4^{2+}$ (TMB = 2,5-dimethyl-2,5-diisocyanohexane) and to $^{1,3}B_2$ excited states in "A-frame"-type complexes (local C_{2v} symmetry) such as $[Ir(\mu\text{-pz})(COD)]_2$ (pz = pyrazolyl, COD = 1,5-cyclooctadiene). Complexes such as these are attractive to study as they are known to luminesce, to undergo photochemical electron transfer, and to serve as powerful one-electron reductants.

Transient difference spectra snd kinetic experiments have been performed on $Rh_2(TMB)_4^{2+}$ in CH_3CN and on $[Ir(\mu\text{-pz})(COD)]_2$ in cyclohexane and 1,2-dichloroethane (DCE) utilizing picosecond transient absorption spectroscopy in order to elucidate the role(s) of the $^{1,3}A_{2u}$ and $^{1,3}B_2$ excited states respectively [128]. Studies on $Rh_2(TMB)_4^{2+}$ [129] show a lifetime of 30 ns for the $^3A_{2u}$ excited state and a fluorescence quantum yield of 4.6×10^{-2}. Difference spectra obtained upon picosecond laser excitation yield $\tau = 820 \pm 20$ ps for the $^1A_{2u}$ excited state [128]. Thus the $^1A_{2u}$ state relaxes to the $^3A_{2u}$ state. The assignment of a $d\sigma^* p\sigma$ electronic configuration to the $^1A_{2u}$ and $^3A_{2u}$ excited states is validated by the dramatically variant difference spectra of the $^1A_{2u}$ and $^3A_{2u}$ states, and by the absence of an intense triplet–triplet absorption band in the 446 nm region. As such, the 440 nm band of the $^1A_{2u}$ state is assigned to a $d\sigma^* \rightarrow p\sigma$ transition [128].

In CH_3CN, $[Ir(\mu\text{-pz})(COD)]_2$ has an emission quantum yield of 8×10^{-3} and a $^3B_2$ excited state lifetime of 250 ns, while the $^1B_2$ excited state has an emission quantum yield of 1×10^{-4} and is shorter lived [126]. A 20–25 ps laser response time appears to be too long to measure the $^1B_2 \rightarrow {}^3B_2$ relaxation process, and no change in transient absorption difference spectra (360–500 nm region) is observed for $[Ir(\mu\text{-pz})(COD)]_2$ in cyclohexane from 0 ps to 11.5 ns after photoexcitation. A lifetime of 2 ps for the $^1B_2$ excited state is expected if similar radiative rates for the $^1A_{2u}$ state of $Ru(TMB)_4^{2+}$ and the $^1B_2$ state are assumed [126].

With regard to quenching mechanisms for the $^1B_2$ and $^3B_2$ excited states of $[Ir(\mu\text{-pz})(COD)]_2$, it is known [130] that the complex undergoes a photo-induced two-electron reduction in DCE (eqn. (12)):

$$[Ir(\mu\text{-pz})(COD)]_2 \xrightarrow[DCE]{h\nu} [Ir(Cl)(\mu\text{-pz})(COD)]_2 + C_2H_4 \qquad (12)$$

The $^3B_2$ luminescence is 40% quenched, and that of the $^1B_2$ state is 30% quenched relative to their luminescence yields in cyclohexane. Absorption difference spectra of $[Ir(\mu\text{-pz})(COD)]_2$ in DCE at $t = 0$ ps and $t = 11.5$ ns after 532 nm ps excitation reveal insignificant differences between the two spectra, with no $^1B_2$ state photochemical reaction products observed during the first 11 ns [128]. Further, relative yields of the $^3B_2$ excited state of this complex (532 nm excitation) were identical, within experimental error, for both the reactive solvent (DCE) and the non-reactive solvent (cyclohexane). From this, one concludes that (i) there is no significant oxidative addition photochemistry emerging from the $^1B_2$ state, (ii) the quantum yield of the $^3B_2$ state is near unity, and (iii) the reduced fluorescence yield in DCE is likely to be due to a slightly more rapid intersystem crossing ($^1B_2 \rightarrow {}^3B_2$) in DCE than in cyclohexane. Winkler et al. [128] suggest that this result may arise from a weak Lewis acid–base pairing of the iridium complex and DCE.

TABLE 9

Quantum yields and lifetimes of the excited states of $[Ir(\mu\text{-}pz')(CO)(PPh_2(O(CH_2)_2R))]_2$ in CH_3CN [a]

R	$^1\phi_{em}$ [b]	$^3\phi_{em}$ [b]	$^1\tau$ (ps)	$^3\tau$ (μs)
$-^+N(C_2H_5)_3$	0.0015	0.034	90	1.25
-H	0.0023	0.025	100	1.11
-py	2.5×10^{-5}	$<10^{-5}$	1.5 [c]	-
-4-Ph-py	$<10^{-5}$	$<10^{-5}$	<1.0 [c]	-

[a] Ref. 131. [b] $\lambda_{exc} = 436$ nm, referenced to $\phi_{em} = 0.06$ for $^*Ru(bpy)_3^{2+}$. [c] Estimated from $^1\phi_{em}$.

Transient absorption and luminescence decay methods have yielded excited state lifetimes of $[Ir(\mu\text{-}pz')(CO)(PPh_2(O(CH_2)_2R))]_2$ ($pz' = 3,5$-dimethylpyrazolyl; R is $^+N(C_2H_5)_3$, H, py, 4-Ph-py) species. When substituent R is a poor electron acceptor (such as H or $^+N(C_2H_5)_3$, the iridium(I) complex luminesces from both the singlet (^1B) and triplet (^3B) $d\sigma^*p\sigma$ excited states. The emission quantum yields and lifetimes are given in Table 9 [131]. The transient difference spectra (Fig. 26) of the singlet and triplet excited states are very similar, with a strong ESA maximum at 390 nm and GSB maximizing at 460 nm. Additional information was obtained by comparing the difference spectra of the complexes where R = py and R = 4-Ph-py with the spectra of the electrochemically generated species $[Ir(\mu\text{-}pz')(CO)(PPh_3)]_2^+$ and of the *N*-alkyl-4-Ph-py$^\cdot$ radical. The authors [131] suggest that electron transfer in the complex with R = 4-Ph-py occurs on a time scale comparable with or shorter than the duration of the laser pulse ($\leqslant 30$ ps). The complex transient species with R = py is thought to be a charge-separated species; the measured rate constants (7.7×10^9 and 1.9×10^{10} s^{-1}) correspond to the electron–hole recombination rates in the complexes with R = py and R = 4-Ph-py respectively. The thermal back electron transfer reactions are about two orders of magnitude slower than the photo-induced electron transfers. The relative rates of the charge-separation and recombination processes in these reactions reflect the interplay among driving force, reorganization energy and donor–acceptor separation [131].

Intramolecular electron transfer in some binuclear complexes has been investigated in complexes of the type $[(NC)_5Fe^{II}\text{–}CN\text{–}Co^{III}(chel)]$, where chel = *N*-benzylethylenediaminetriacetato (NBETA) and *N*-hydroxyethylethylenediaminetriacetato (HEDTA), by Rentzepis and coworkers [132] using picosecond absorption spectroscopy. The reduction of $Fe(CN)_6^{3-}$ by $Co(EDTA)^{2-}$ proceeds [133,134] via the mechanism outlined in Scheme 2. The $Fe^{III}(CN)_6^{3-}$ complex also reacts with Co^{II}(HEDTA) and Co^{II}(NBETA) at pH 6 to give $[(NC)_5Fe^{II}\text{–}CN\text{–}Co^{III}(HEDTA)]$ and $[(NC)_5Fe^{II}\text{–}CN\text{–}$

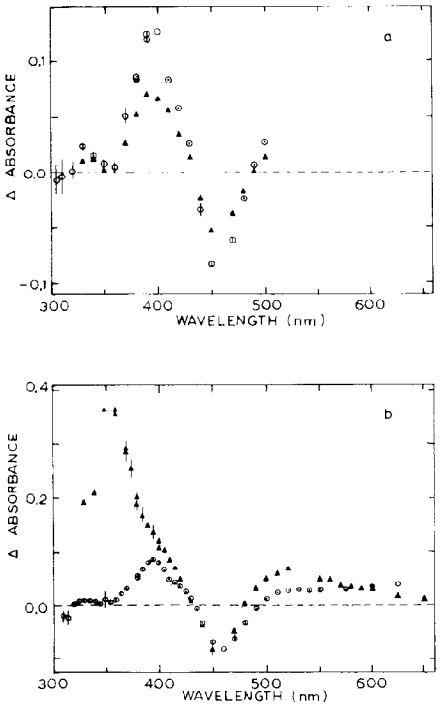

Fig. 26. Transient difference spectra of $[Ir(\mu\text{-pz}')(CO)(PPh_2(O(CH_2)_2R))]_2$ complexes in CH_3CN following 30 ps excitation: (a) R = H, and (b) R = py (○) and R = 4-Ph–py (▲) (from ref. 131).

Co^{III}(NBETA)] respectively [135]. Previous attempts [136] to measure the inner-sphere rate of electron transfer, k_{et}, of $[(NC)_5Fe^{II}–CN–Co^{III}$(chelate)]-type complexes were ineffectual using conventional stopped-flow and temperature-jump techniques.

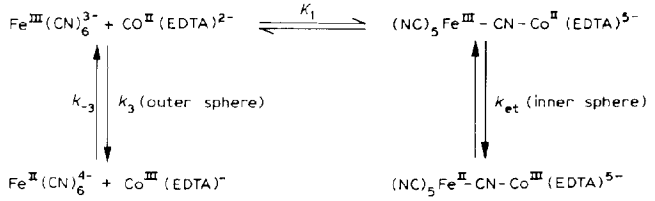

Scheme 2

Picosecond laser (6 ps pulses) photoexcitation with 530 nm light excites the $^1T_{1g} \leftarrow {}^1A_{1g}$ $(t_{2g})^5(e_g)^1 \leftarrow (t_{2g})^6$ transition in $[Co^{III}$(chel)]$^-$ or

$[(NC)_5Fe^{II}-CN-Co^{III}(chel)]^{4-}$; relaxation back to the ground state occurs in less than 6 ps. In contrast, reversible transient bleaching is evident for $[(NC)_5Fe^{II}-CN-Co^{III}(chel)]^{4-}$ and persists for more than 500 ps. The bleaching recovery process is accompanied by a fast (< 10 ps) rise in the 420 nm transient absorption; this absorption decays exponentially with a half-life of ca. 150 ps. The kinetic results obtained in this study are identical, within experimental error, for chel = HEDTA and NBETA. Transient absorption difference spectra (λ_{exc} = 532 nm; 25 ps FWHM pulses) of $[(NC)_5Fe^{II}-CN-Co^{III}(HEDTA)]$ in the 400–470 nm wavelength window are identical at 25 and 125 ps subsequent to excitation. An alteration in absorption maxima materializes at 420 nm, with a profile similar to that of the $Fe^{III}(CN)_6^{3}$ spectrum; bleaching occurs at longer wavelengths, resulting in an isosbestic point at 448 nm. Scheme 3 (eqns. (13)–(17)) has been proposed [132] to accommodate these experimental results.

$$Fe^{II}-CN-Co^{III} \xrightarrow{h\nu} Fe^{II}-CN-Co^{III*} \quad \text{(excitation)} \quad (13a)$$

or

$$Fe^{II}-CN-Co^{III} \xrightarrow{h\nu} Fe^{III}-CN-Co^{II**} \quad \text{(excitation)} \quad (13b)$$

$$Fe^{II}-CN-Co^{III*} \rightarrow Fe^{III}-CN-Co^{II**} \quad (< 10 \text{ ps}) \quad (14)$$

$$Fe^{III}-CN-Co^{II**} \rightarrow Fe^{III}-CN-Co^{II} \quad (\sim 75 \text{ ps}) \quad (15)$$

$$Fe^{III}-CN-Co^{II} \rightarrow Fe^{II}-CN-Co^{III*} \quad (\sim 95 \text{ ps}) \quad (16)$$

$$Fe^{II}-CN-Co^{III*} \rightarrow Fe^{II}-CN-Co^{III} \quad (> 500 \text{ ps}) \quad (17)$$

Scheme 3

In this Scheme, two options present themselves for the initial excitation process. First, excitation of $^1A_{1g} \rightarrow {}^1T_{1g}$ for Co^{III} to produce $^*Co^{III}$ having an unfilled low lying t_{2g} orbital (i.e. $(t_{2g})^5(e_g)^1$) (eqn. (13a) would increase the Co^{III} electron affinity, thereby causing electron transfer to occur (eqn. (14)). However, direct excitation of $Fe^{II}-CN-Co^{III}$ to the CT band at 530 nm would result in the direct formation of $Fe^{III}-CN-Co^{II**}$ (eqn. (13b)) to give the Fe^{III} absorption and Co^{II} in the ^2E $((t_{2g})^6(e_g)^1)$ state. Such a pathway is plausible if one assumes the presence of a CT band in the 500–600 nm region, as has been assigned [137] in an Ru–Ru binuclear complex. Equation (15) shows the cobalt doublet-to-quartet spin flip which would accompany a $t_{2g} \rightarrow e_g$ transition to the high spin Co^{II} $^4T_{1g}$ $((t_{2g})^5(e_g)^1)$ state; a spin-allowed electron-transfer back reaction (eqn. (16)) occurs in about 95 ps. Thus, the Co^{III} is in an excited $^3T_1$ or $^3T_2$ $((t_{2g})^5(e_g)^1)$ state and can slowly decay to the ground singlet state (eqn. (17)). Intersystem crossing cannot be observed directly owing to the low extinction coefficients of Co^{II}.

In the $[(NC)_5Fe^{II}-CN-Co^{III}(chel)]$ system and in other bimetallic ruthenium complexes, electron transfer is thought to proceed via resonance transfer between metal centers with some influence from the bridging ligands [138,139]. This type of mechanism is ruled out for the $Fe^{II}-CN-Co^{III}$ system because the MLCT ($Fe^{II} \rightarrow CN$) transition occurs in the near-UV region [132].

F. SPECTROSCOPY OF METALLOPORPHYRIN COMPLEXES

Understanding the photochemical and photophysical characteristics of metalloporphyrins is important for several reasons. First, such complexes may be considered as models of hemoproteins that activate molecular oxygen [140,141]. These complexes can serve as mediators in biochemical redox reactions [142–144], and may act as precursors in the preparation of one-dimensional electrical conductors [145]. Additionally, it is suggested [146–150] that metalloporphyrins could serve as photosensitizers in light-harvesting systems for solar energy conversion and storage, since they absorb light strongly in the visible, and often in the near-IR spectral regions. Also, investigations have shown [151,152] that cofacially joined metalloporphyrins and free-base porphyrins can act as functioning models of the primary electron-transfer couple of Photosystem II of green plants.

Generally speaking, those porphyrins not possessing a metal and those complexed with closed-shell diamagnetic metal ions, e.g. magnesium(II), zinc(II), exhibit strong fluorescence with decay times slower than those of other metalloporphyrins. Metalloporphyrins incorporating open-shell diamagnetic metal ions, e.g. palladium(II), platinum(II), tend to fluoresce slightly, though they usually phosphoresce strongly. In contrast, metalloporphyrins formed with paramagnetic metals, e.g. iron(II), copper(II), show no fluorescence and only slight phosphorescence.

(i) Molybdenum(V)

The chemistry of early transition metals in high oxidation states, e.g. molybdenum(V), is dominated by the presence of very strong M=O bonding. Serpone et al. [153] have examined the electronic relaxation processes in (5,10,15,20-tetraphenylporphyrinato)oxomethoxomolybdenum(V), OMo(TPP)OCH_3, a molybdenum(V) d^1 porphyrin complex by pisosecond transient absorption spectroscopy.

Ground state OMo(TPP)OCH_3 is monomeric in CH_2Cl_2 [145,154] and contains molybdenum(V) as determined from magnetic susceptibility [155] and ESR [154–156] measurements. Ground state absorption bands in

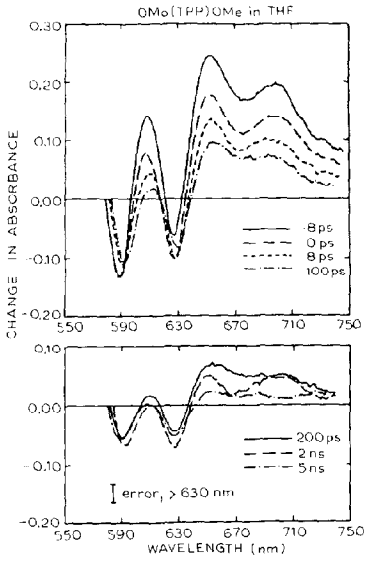

Fig. 27. Plots of change in absorbance vs. wavelength for THF solutions of OMo(TPP)(OCH_3) at the indicated delay times after 532 nm laser excitation (6 ps pulses) (from ref. 153).

CH_2Cl_2 (and THF) occur at 538 (536), 580 (579), 621 (618), and 675 (645) nm, in good agreement with literature values [145,157]. Thus in THF the $OMo(TPP)OCH_3$ complex is thought to be monomeric. The ground state is a doublet, $^2S_0$; the unpaired d_{xy} electron interacts with the lowest energy ($\pi\pi^*$) excited states to create several new states: $^2S_1(\pi\pi^*)$, $^2T_1(\pi\pi^*)$ and $^4T_1(\pi\pi^*)$ [146,158].

Picosecond absorption spectra (527 nm, 6 ps FWHM pulses) of $OMo(TPP)OCH_3$ in THF (Fig. 27) show ESA bands with maxima at ~ 605, ~ 650 and ~ 700 nm, and GSB bands with maxima at ~ 590 and ~ 630 nm. A kinetic analysis of ΔA vs. time plots at 650 nm yields an apparent decay time of 12 ± 4 ps and a second decay time of 4 ± 1 ns. The 12 ps lifetime is indistinguishable from the instrument response limited decay time (9 ± 3 ps); thus a 2–9 ps lifetime was assigned [153] to this excited state species. Furthermore, this excited state relaxes with high yield (> 50%) to the longer-lived (4 ± 1 ns) excited state or photoproduct, as indicated by the substantial decay of the first ESA within 100 ps of excitation at about 600 nm and at above 640 nm with very little decay in the ground state bleaching regions of the spectrum.

On the basis of the above observations and assignments (see, for example, ref. 146), Serpone et al. [153] have proposed the decay scheme summarized in eqns. (18)–(20):

$$^2S_0 \xrightarrow{h\nu} {}^2S_1(\pi\pi^*) \rightarrow {}^2T_1(\pi\pi^*)(\tau < 2 \text{ ps; not observed}) \quad (18)$$

$$^2T_1(\pi\pi^*) \rightarrow \left({}^4T_1(\pi\pi^*) \rightleftharpoons {}^2T_1(\pi\pi^*)\right)(\tau \approx 2\text{–}9 \text{ ps}) \quad (19)$$

$$\left({}^4T_1(\pi\pi^*) \rightleftharpoons {}^2T_1(\pi\pi^*)\right) \rightarrow {}^2S_0(\tau \approx 4 \text{ ns}) \quad (20)$$

Its credence, however, awaits precise methods of calculating CT state energies. Very likely, the 2–9 ps lifetime corresponds to the equilibration of the $^2T_1(\pi\pi^*)$ and $^4T_1(\pi\pi^*)$ states (eqn. (19)); the longer-lived (4 ns) transient reflects the decay of the $^4T_1 \rightleftharpoons {}^2T_1$ equilibrium distribution (eqn. (20)). The initially populated $^2S_1(\pi\pi^*)$ state is known to be emissionless in molybdenum(V) porphyrin complexes [146], and was not observed in this investigation (eqn. (18)) [153].

(ii) Osmium(II)

Interest in studying osmium porphyrin complexes arises from the following: (i) their close relationship to the biologically important iron(II) porphyrins found in hemoglobin, cytochrome P450 and other redox catalysts; (ii) the observation that these complexes are kinetically inert relative to hemochrome complexes, and thus are useful model compounds for the iron(II) porphyrins; (iii) the fact that these complexes possess unique electrochemical properties rendering them useful for photochemical electron transfer studies.

The metal ions iron(II), ruthenium(II) and osmium(II) all have an nd^6 electron configuration. A knowledge of the bonding and π-backbonding relationships in iron(II) and osmium(II) porphyrin complexes should prove helpful in mechanistic studies. The shortcomings with iron(II) porphyrins center on the ligand-field splitting not being large enough to shift the ligand-field (dd) states above the ($\pi\pi^*$) states of the porphyrin ring, thus complicating somewhat the low energy states in the iron(II) complexes. The osmium(II) porphyrins are better models of iron(II) porphyrins than are the ruthenium(II) porphyrins inasmuch as the energies of the d_{xy}, d_{xz} and d_{yz} orbitals are nearly the same for the osmium(II) and iron(II) species [159]. The d orbitals of osmium(II) extend further into space than those of iron(II), and thus the π-backbonding effects will be more pronounced for osmium than for iron porphyrins.

The absorption and emission spectra of a free-base porphyrin are best understood in terms of their highest occupied orbitals, $a_{2u}(\pi)$ and $a_{1u}(\pi)$,

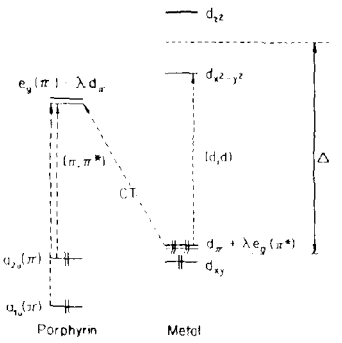

Fig. 28. Schematic illustration of important orbitals for spectra of d^6 six-coordinate porphyrins (from ref. 159).

and of their lowest unoccupied orbitals, $e_g(\pi^*)$. Hence, when an nd^6 metal complexes with a porphyrin, the interaction between the free-base porphyrin orbitals and the metal d orbitals becomes important. The important orbitals for an nd^6 six-coordinate metalloporphyrin are illustrated in Fig. 28. The nature of the axial ligands (along the z axis of the metalloporphyrin) leads either to an enhancement or to a decrease in metal–porphyrin interactions. For strong σ-donor ligands in these positions (e.g. PMe_3, NMe_3) the filled d obitals of osmium(II) (d_{xy}, d_{xz}, d_{yz}) lie above the $a_{2u}(\pi)$ and $a_{1u}(\pi)$ porphyrin orbitals [159] giving rise to π backbonding between the osmium(II) $d\pi$ orbitals and the porphyrin empty $e_g(\pi^*)$ orbitals, which would raise the energy of the latter orbitals relative to their energy in a free-base porphyrin. Also, forbidden CT transitions, $e_g(d\pi) \rightarrow e_g(\pi^*)$, will lie lower in energy than the allowed $(\pi\pi^*)$ states. For π-acceptor ligands, e.g. py, CO, NO^+, the backbonding of the $d\pi$ electrons will shift from equatorial to axial [159], and both the filled d and the empty $e_g(\pi^*)$ orbitals shift to lower energy. Consequently, the $(\pi\pi^*)$ absorption is expected to be red shifted; the lowest energy excited state is expected to change from $(d\pi,\pi^*)$ ($d\pi = d_{xz}$, d_{yz}) to $(\pi\pi^*)$, and the first oxidation potential to be more positive.

Several osmium(II) porphyrin complexes have been examined by Serpone, Netzel and their coworkers [160,161]. Picosecond laser flash photolysis (527 nm, 6 ps FWHM pulses) was used to examine Os(OEP)LL′, where OEP = octaethylporphyrin, L and L′ = py (pyridine), NO, $P(OMe)_3$ or L,L′ = CO, py or NO, OMe. The objectives of the study were (i) to detect the relaxation of the singlet excited states and ascertain how this was affected by the nature of the lowest energy excited states, and (ii) to determine whether the spectra of the excited states were dependent on their identity, e.g. $(d\pi,\pi^*)$ or $(\pi\pi^*)$. A general decay scheme for the low lying excited states of

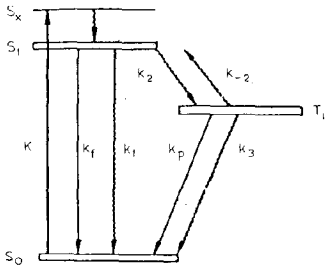

Fig. 29. Decay scheme for low lying excited states of osmium(II) porphyrins (from ref. 160).

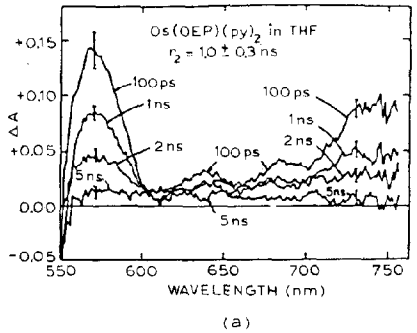

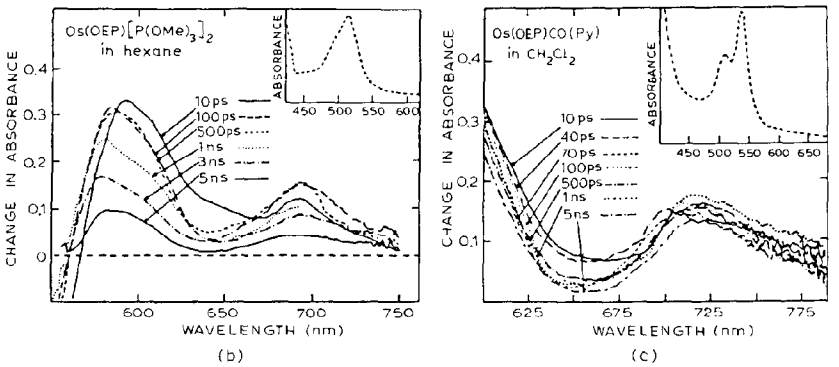

Fig. 30. Change-in-absorbance spectra of osmium(II) octaethylporphyrins possessing low lying $d\pi,\pi^*$ states, on excitation with the second harmonic of an Nd : glass laser (6 ps pulses) (from refs. 160 and 161).

osmium(II) porphyrins is given in Fig. 29. The Os(OEP)LL′ complexes do not fluoresce, so that k_f is insignificant and the decay of S_1 is therefore set by $\tau(S_1) = (k_1 + k_2)^{-1}$. The low values observed for the phosphorescence quantum yield ϕ_P of Os(OEP)(NO)(OMe) and Os(OEP)O_2 [159], and the assumption that the triplet yield, $\phi(T_1) = k_2/(k_1 + k_2)$, should be greater than ϕ_P in complexes containing the heavy osmium atom, imply that $k_P \ll k_3$. Further, k_{-2} is likely to be negligible since the energy gap $E(S_1) - E(T_1)$ is considerably greater than $k_B T$, the Boltzmann energy [159]. Two transient decays are expected; one corresponding to S_1 decaying to S_0 and T_1 with $\tau(S_1) = (k_1 + k_2)^{-1}$, and the other corresponding to T_1 returning to the S_0 ground state with $\tau(T_1) = k_3^{-1}$.

The osmochromes having $(d\pi,\pi^*)$ lowest energy excited states included Os(OEP)[P(OMe)$_3$]$_2$, Os(OEP)CO(py) and Os(OEP)(py)$_2$, while those hav-

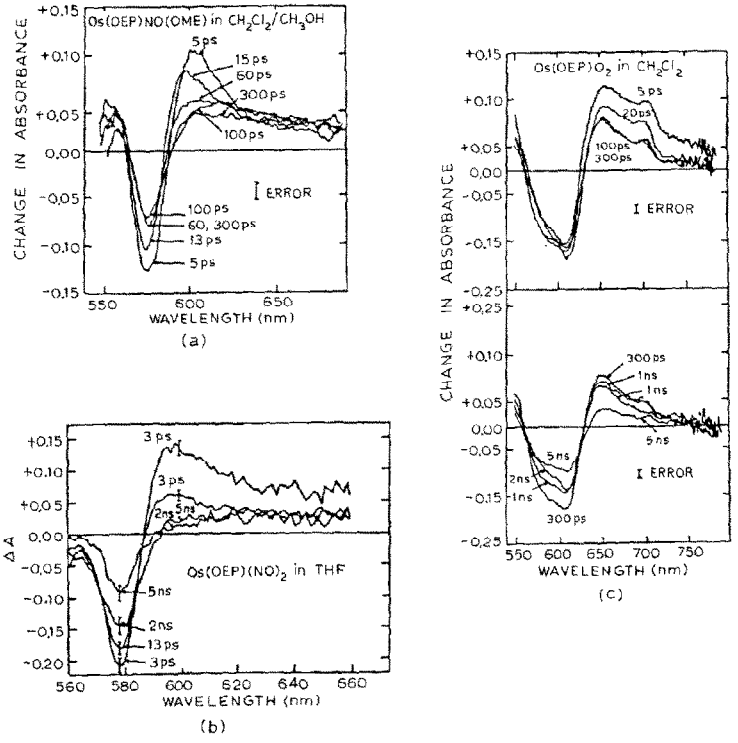

Fig. 31. Change-in-absorbance spectra for osmium(II) octaethylporphyrins possessing low lying $\pi\pi^*$ states, on excitation with the second harmonic of an Nd:glass laser (6 ps pulses) (from refs. 160 and 161).

TABLE 10

Kinetic observations in the photophysics of osmium(II) porphyrins Os(OEP)LL′ [a]

(A) ($d\pi,\pi^*$) states

$Os(OEP)(py)_2$	$Os(OEP)[P(OMe)_3]_2$	Os(OEP)CO(py)
(a) $S_1 \rightarrow T_1 + S_0$ (?%) ($\leqslant 9$ ps)	$S_1 \rightarrow T_1 + S_0$ ($\sim 20\%$) ($\leqslant 9$ ps)	$S_1 \rightarrow T_1 + S_0$(?%) ($\sim 50$ ps)
(b) $T_1 \rightarrow S_0$ (~ 1 ns)	$T_1 \rightarrow S_0$ (~ 6 ns)	$T_1 \rightarrow S_0$ (~ 16 ns)

(B) ($\pi\pi^*$) states

Os(OEP)(NO)(OMe)	$Os(OEP)(NO)_2$	$Os(OEP)O_2$
(a) $^1(\pi\pi^*) \rightarrow {}^1(\pi\pi^*)^{\neq}$ (~ 15 ps)	–	–
(b) $^1(\pi\pi^*)^{\neq} \rightarrow {}^3(\pi\pi^*) + S_0$ ($\sim 40\%$) (~ 36 ps)	$^1(\pi\pi^*) \rightarrow {}^3(\pi\pi^*) + S_0$ ($\sim 50\%$) (~ 9 ps)	$^1(\pi\pi^*) \rightarrow {}^3(\pi\pi^*) + S_0$ (0%) (~ 13 ps)
(c) $^3(\pi\pi^*) \rightarrow S_0$ (~ 5 ns)	$^3(\pi\pi^*) \rightarrow S_0$ (~ 9 ns)	$^3(\pi\pi^*) \rightarrow S_0$ (~ 6 ns)

[a] Refs. 160 and 161.

ing ($\pi\pi^*$) lowest excited states are Os(OEP)(NO)(OMe), $Os(OEP)O_2$ and $Os(OEP)(NO)_2$. Results from analyses of the transient absorption spectra and difference spectra (Figs. 30 and 31) obtained upon irradiation of Os(OEP)LL′ with 527 nm light from a 6 ps pulsed Nd : glass laser are shown in Table 10 [160,161]. Similar transient absorption spectra were obtained for the complexes containing LL′ = $(py)_2$, $[P(OMe)_3]_2$ and (CO)(py). The bands observed in the 700–750 nm region are due to excited state absorption of the T_1 state of ($d\pi,\pi^*$) character, and the spectra support the prediction of the backbonding model that the ($d\pi,\pi^*$) states lie lower in energy than the ($\pi\pi^*$) states. The decidedly different profile of the S_1 and T_1 excited states of complexes with LL′ = (NO)(OMe), O_2 and $(NO_3)_2$ support the assignment of the T_1 state of these complexes to ($\pi\pi^*$).

(iii) Palladium(II)

Picosecond laser excitation (530 nm, 6 ps pulses) of palladium(II) protoporphyrin IX dimethyl ester in benzene results in the formation of an intermediate which absorbs at 430 nm [162]. The decay of this species is biphasic: $\tau = 19 \pm 3$ ps for the short-lived component and $\tau > 1$ ns for the second transient. Similar behavior was observed for absorbance changes at 560 nm; however, the principal change here arises from GSB. Ground state recovery also follows biphasic kinetics: $\tau = 18 \pm 3$ ps for the short-lived

component and $\tau > 1$ ns for the long-lived component. The results are consistent [162] with the existence of two transients, one with a lifetime of 19 ± 3 ps and the other with a lifetime greater than 1 ns. On the basis of the weak fluorescence ($\phi_F = 1\text{–}3 \times 10^{-4}$ for palladium(II) porphyrins [163]), strong phosphorescence, the presence of a heavy atom and the above data for palladium(II) protoporphyrin, the short-lived transient is likely to be the lowest singlet excited state of the porphyrin.

Preliminary studies of Pd(OEP) in methylmethacrylate using a mode-locked Nd : glass laser (530 nm, ca. 5 ps pulses) show that the T_1 transient absorbs more light than the S_1 transient, and that the entire spectrum is slightly blue shifted relative to that of $Sn(OEP)Cl_2$ [158].

(iv) Platinum(II)

For the platinum(II) protoporphyrin IX dimethyl ester in benzene, a transient absorption at 480 nm and bleaching at 550 nm were observed under similar conditions. The lifetime of the absorption at 480 nm and the recovery lifetime at 550 nm are similar. The species responsible for the transient absorption is the lowest excited triplet state T_1 populated via rapid intersystem crossing from the lowest excited singlet state S_1 [162]. The failure to observe two transient species is due to a very short-lived excited singlet state S_1. Inasmuch as the absorbance difference between S_1 and T_1 is less than 0.02 in the platinum porphyrin (compared with 0.07 in the palladium porphyrin), and assuming similar differences in absorption cross-section between S_1 and T_1 for the platinum and palladium complexes, a lifetime of 1.7 ps has been estimated, much shorter than the excitation pulse width [162].

Transient absorption spectroscopy of Pt(OEP) in THF (Fig. 32) reveals two transients: a transient with a lifetime of $\leqslant 15$ ps assigned to $S_1(\pi\pi^*)$, and a second less strongly absorbing transient with a lifetime greater than 50 ns, assigned to $T_1(\pi_p^*)$ are observed in the short-wavelength region (550–670 nm). In the longer-wavelength region ($\lambda \geqslant 720$ nm), the T_1 transient appears to absorb more strongly [161]. This wavelength relationship has been observed for the $S_1(\pi\pi^*)$ and $T_1(\pi\pi^*)$ excited states of free-base octaethylporphyrin (H_2OEP) [164]. The lifetime of the T_1 transient species of Pt(OEP) ($\tau > 50$ ns) agrees in principle with the room temperature lifetime of 63 μs for the T_1 state of platinum etioporphyrin I [163]. Insofar as the fluorescence quantum yield of platinum porphyrin is less than 2×10^{-5}, and since the radiative lifetime of its S_1 state is ca. 60–70 ns, its lifetime should be less than 1.5 ps. A lower limit of 0.7 ps for the S_1 lifetime of platinum porphyrin has been inferred from quasi-line spectra of the $Q(0,0)$ band in *n*-octane at 77 K [163]. Thus, an S_1 lifetime of 1 ps for Pt(OEP) is consistent with that

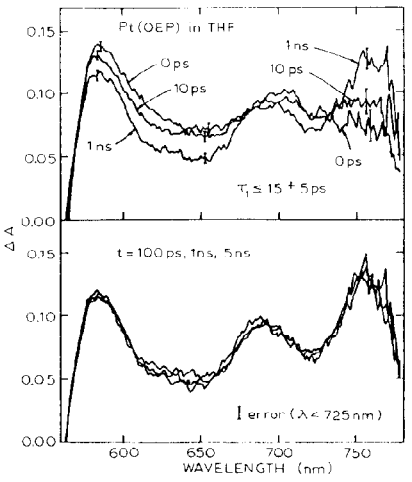

Fig. 32. Change-in-absorbance vs. wavelength for PtOEP in THF at the indicated delay times after phtoexcitation with the second harmonic of an Nd:glass laser (6 ps pulses) (from ref. 161).

for other platinum porphyrin complexes, and is also consistent with the observation of $^1(\pi\pi^*)$ states in $5d$ metalloporphyrins, as has been observed for some Os(OEP)LL′ complexes, and is not unique to the latter complexes. Further, the differences between osmium porphyrins with $T_1(\pi\pi^*)$ excited states and platinum porphyrins are probably due to axial ligand influences.

(v) Zinc(II)

Zinc(II) protoporphyrin IX dimethyl ester in benzene exhibits strong excited state absorption at 480 nm and ground state bleaching at 560 nm upon picosecond laser excitation (6 ps pulses) at 530 nm. Both processes have the same time constant (2.6 ± 0.5 ns) which agrees well with the lifetime of the excited singlet state for Zn(TPP) [165], Zn(*o*-methylTPP) [165] and Zn(etioporphyrin) [165], as estimated from natural lifetimes and quantum yields. Also, the time constant of 2.6 ns is similar to the value for the observed fluorescence lifetimes of Zn(mesoporphyrin) [166] and Zn(TPP) [166].

(vi) Nickel(II)

Upon picosecond laser excitation (6 ps pulse) at 530 nm, nickel(II) protoporphyrin IX dimethyl ester in benzene gives rise to a transient

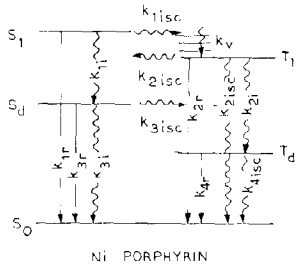

Fig. 33. Schematic energy level diagram for nickel protoporphyrin IX dimethyl ester. (from ref. 162).

absorption at 480 nm, displaying biphasic kinetic behavior. The decay time associated with the short-lived component is 10 ± 2 ps, while that of the longer-lived component is 250 ± 60 ps [162]. In contrast with the palladium(II) protoporphyrin IX dimethyl ester complex, the decay kinetics are monophasic for the bleaching observed at 560 nm with a recovery time of 270 ± 20 ps which correlates well with the transient decay time of 480 nm.

Theoretical calculations by Maki [167] and Ake and Gouterman [168] have led to the suggestion of a lower lying triplet level, $^3B_{1g}$, for coordination compounds of nickel. Further, its existence is corroborated by quenching studies [169,170]. According to Adamczyk and Wilkinson [169] the $^3B_{1g}$ triplet state is thought to lie lower than 8000 cm^{-1} above the ground state, while calculations by Ake and Gouterman [168] and estimates from the nickel(II) protoporphyrin IX dimethyl ester absorption spectrum would put the $^1B_{1g}$ state approximately 9000 cm^{-1} above the ground state. If these calculations are exact, the $^1B_{1g}$ level should lie much lower than the lowest ($\pi\pi^*$) excited singlet state ^1A (Fig. 33). Kobayashi et al. [162] have submitted three tentative assignments for the two components observed in the transient absorption spectrum of nickel(II) protoporphyrin IX dimethyl ester: (i) the short-lived component corresponds to the S_1 (^1A) state, and the long-lived component corresponds to the S_4 ($^1B_{1g}$) state; (ii) the short-lived component correlates with the S_d ($^1B_{1g}$) state, while the long-lived component correlates with the T_d ($^3B_{1g}$) state; (iii) the short-lived component is identified with the T_1 ($\pi\pi^*$) state, while the long-lived component is identified with the T_d ($^3B_{1g}$) state. Assignments (ii) and (iii) were discounted on the basis of Franck–Condon factors for the T_1–S_0 and S_d–S_1 energy gaps. However, energy gap considerations (S_d–S_1) do favor assignment (i), inasmuch as a time constant of 10 ps for $S_1 \rightarrow S_d$ internal conversion appears reasonable. The absence of luminescence from nickel porphyrins can also be rationalized in terms of assignment (i), since the very rapid

$S_1 \rightarrow S_d$ internal conversion quenches the fluorescence. The internal conversion process diminishes T_1 phosphorescence. Fluorescence from the S_d state is expected, but is likely to be located in the IR region and/or its quantum yield is small, thus rendering its detection difficult.

Several photochemical studies have been carried out by Tsvirko et al. [170] on nickel octamethylporphyrin, nickel etioporphyrin and Ni(TPP) in an effort to determine whether the T_1 state is indeed populated. The observation of the quenching of palladium etioporphyrin phosphorescence with increasing nickel porphyrin concentration, and the absence of nickel porphyrin phosphorescence upon excitation of palladium etioporphyrin favors the hypothesis in which the T_1 state of the nickel(II) porphyrin is populated but its lifetime is very short. Such results cannot, however, be taken to mean that excitation into a singlet state of the nickel porphyrin leads to relaxation to a triplet state. The experimental results on nickel protoporphyrin IX dimethyl ester would seem to suggest that the T_1 state is not appreciably populated on excitation to S_1; the S_d state affords the major relaxation pathway.

In comparing the nickel, palladium and platinum porphyrins, it is noteworthy that palladium porphyrins are weakly fluorescent, while nickel and platinum are non-fluorescent. The differences between the palladium and platinum porphyrin observations can be understood in terms of the strong effect of the heavier Pt atom. However, this rationale does not hold for nickel, the lightest metal of the triad. The behavior of nickel protoporphyrin IX dimethyl ester suggests that rapid internal conversion occurs from S_1 to the intermediate S_d state (see Fig. 33), and that the S_d ($^3B_{1g}$) state is governed by nickel d electrons [162].

In palladium, platinum and zinc porphyrin systems, it has been established that the $S_1 \rightarrow S_0$ internal conversion process is negligible, so that $(k_{isc})^{-1}$ for $S_1 \rightarrow T_1$ corresponds to the observed S_1 lifetime. For the nickel, palladium and platinum protoporphyrin IX dimethyl ester systems, k_{isc}^{1} for $S_1 \rightarrow T_1$ follows the order of atomic number Z: $\tau > 10$ ps (nickel), 19 ± 3 ps (palladium), $\ll 8$ ps (platinum).

(vii) Copper(II), silver(II)

In general, paramagnetic metalloporphyrin complexes such as copper, silver and gold either exhibit no emission, or as with copper, reveal a short-lived phosphorescence. The central metal atom performs an important role in the electronic energy relaxation rate of porphyrin complexes, which decay via radiative and non-radiative decay processes. Figure 34 presents a schematic energy level diagram of copper(II) and silver(II) porphyrin complexes. It has been established [171] that the singlet states in these complexes

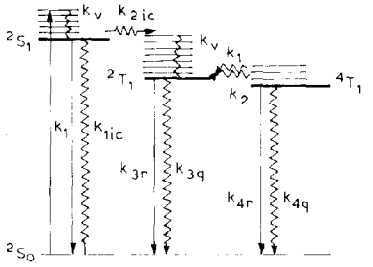

Fig. 34. Schematic energy level diagram for copper and silver porphyrins (from ref. 172).

couple with doublet levels to form "singdoublets" ($^2S_1$), and triplets couple with doublets to form "tripdoublets" ($^2T_1$) and "tripquartet" ($^4T_1$) states. The existence of such states has been supported by phosphorescence lifetime measurements to give a characteristic lifetime from the equilibrium state of "tripdoublet" and "tripquartet".

Picosecond laser (6 ps pulses) excitation of copper(II) protoporphyrin IX dimethyl ester in benzene gives rise to a transient absorption at 430 nm, which decays in a biphasic manner [172]. The short-lived component has a time constant of 450 ± 50 ps; the longer-lived component has a lifetime > 1 ns. Decay of the 480 nm transient is concomitant with decay of ground state bleaching; the decay time constants are 460 ± 50 ps and > 1 ns. Similar results were obtained for copper(II) protoporphyrin IX dimethyl ester in ethyl iodide, indicating that there is no heavy atom effect in this system.

To account for the observed behavior, Kobayashi et al. [172] have suggested that upon excitation of this copper porphyrin, a state I is formed from the Franck–Condon state of the excited copper complex. The state I relaxes with a time constant of > 1 ns. The authors propose that state I corresponds to $^2T_1$ and the other state (II) corresponds to $^4T_1$ states (Fig. 34); $k_1 = 1.6 \times 10^9$ s^{-1}, $k_2 = 0.56 \times 10^9$ s^{-1} and $k_{2\,ic} > 1.6 \times 10^{11}$ s^{-1}.

Results of picosecond laser excitation (530 nm) of silver(II) protoporphyrin IX dimethyl ester in benzene are very similar to those of the copper(II) analog [172]. The decay of the transient absorption at 480 nm is probably biphasic as is decay of GSB at 570 nm; however, the ΔA values were too small at longer times to ascertain the decay of the longer-lived component. Plots of absorbance changes vs. time give decay times of 12 ± 2 ps for the short-lived component of the 480 nm transient absorption, and 11 ± 2 ps for the bleaching decay at 570 nm [172]. Computation yields $k_1 = (6\text{–}8) \times 10^{10}$ s^{-1} and $k_2 = (2\text{–}2.7) \times 10^{10}$ s^{-1}, using arguments similar to those for the copper(II) system. It is noteworthy that the time constants of the short-lived (absorption and bleaching) components of the silver complex are a factor of 40 longer than those of the analogous copper(II)

complex, and the k_1 and k_2 values are about 40 times larger in the silver(II) system than in the copper(II) system. This suggests the possibility of the metal Z number operating in the relaxation process.

Both nickel(II) protoporphyrin IX dimethyl ester and its silver(II) analog are non-fluorescent and non-phosphorescent. These properties of the nickel(II) system can be rationalized in terms of a high $S_1 \rightarrow T_1$ intersystem crossing rate and the high rate of $T_1 \rightarrow T_d$ internal conversion (see Fig. 33). Applying this to the silver(II) porphyrin, interaction between the low lying $d\,d$ triplet state and the ground state generates the low lying tripdoublet (^2T_d) and tripquartet (^4T_d) states. Relaxation occurs from $^2T_1$ to ^2T_d and from $^4T_1$ to ^5T_d, with rapid internal conversion from $^2S_1$ to $^2T_1$. Alternatively, the $^2T_1$ and $^5T_1$ states are equilibrated and subsequently relax non-radiatively to a $^2(d\pi^*)$ CT doublet state. Antipas et al. [173] have employed metal redox potential techniques, near-IR absorption spectra and iterative extended Hückel calculations to show that there is a charge-transfer doublet state $^2(d\pi^*)$ lower in energy than the $^2(\pi\pi^*) \equiv {}^2T_1$ state in silver(II) porphyrins. For the silver(II) protoporphyrin IX dimethyl ester system, then, the time constant > 1 ns could correlate with the $^2T_1 \rightarrow {}^2(d\pi^*)$ process, or the 12 ps process corresponds to the $^2T_1 \rightarrow {}^2(d\pi^*)$ process and the > 1 ns time constant to the $^2(d\pi^*) \rightarrow {}^2S_0$ process.

In summary, excitation of copper(II) protoporphyrin IX dimethyl ester results in the population of the $^2S_1$ Franck–Condon state, which decays to $^2T_1$ within 8 ps. The $^2T_1$ state relaxes to a $^2T_1$ and $^4T_1$ equilibrium state with a time constant of 450–460 ps. Phosphorescence occurs from this equilibrium state. From silver(II) protoporphyrin IX dimethyl ester, excitation leads to $^2S_1$ Franck–Condon population, followed by relaxation to $^2T_1$ within 8 ps. The $^2T_1$ and $^4T_1$ states are equilibrated with a time constant of 11–12 ps and subsequently relax non-radiatively to ^2T_d and ^4T_d, or to the $^2(d\pi^*)$ state [172].

Picosecond excitation (530 nm; ca. 5 ps pulses) of Cu(OEP) and Cu(TPP) in benzene at room temperature results in strong and broad absorption in the blue region extending to 530 nm with a maximum at 430 nm [158]. However, for both complexes, only one transient absorption is seen, implying that changes corresponding to $^2T_1 \rightarrow {}^4T_1$ (see Fig. 34) are not observed. It was suggested that perhaps the spectra of $^2T_1$ and $^4T_1$ are very similar inasmuch as they differ only in the coupling of the excited π system of the unpaired d electron.

G. CONCLUDING REMARKS

The examples that have been briefly examined here attest to the powerful utility of picosecond transient emission and transient absorption techniques

using high power or low power mode-locked lasers and fast detection methods to unravel the primary events in many chemical processes occurring in transition metal photochemistry. The technological advances made in picosecond spectroscopy have made it possible for the photochemist to elucidate and understand to a greater degree than before transient chemical intermediates and kinetics of primary events in photochemical reactions, as well as processes that are particularly relevant to photocatalysis and to semiconductors. The more recent advent of subpicosecond instrumentation and spectroscopic techniques promises further interesting probes of the events occurring immediately following the interaction between photons and light absorbers (molecules).

Inevitably, as in any young and complex area as that discussed in this article, which seeks to understand the early events in a photochemical reaction, controversies will arise. We view this as a healthy sign of the interest and progress we make in our collective understanding of chemical processes.

ACKNOWLEDGEMENTS

Our work is supported by the Natural Science and Engineering Research Council of Canada. We are also grateful to the various publishers of journals for their kind permission to reproduce some of the figures.

REFERENCES

1 J. Nasielski and A. Colas, Inorg. Chem., 17 (1978) 237.
2 J. Nasielski and A. Colas, J. Organomet. Chem., 101 (1975) 215.
3 J.K. Burdett, Coord. Chem. Rev., 27 (1978) 1.
4 J.J. Turner, J.K. Burdett, R.N. Perutz and M. Poliakoff, Pure Appl. Chem., 49 (1977) 227.
5 R.N. Perutz and J.J. Turner, J. Am. Chem. Soc., 97 (1975) 4791.
6 J.K. Burdett, J.M. Grzybowski, R.N. Perutz, J.J. Turner and R.F. Turner, Inorg. Chem., 17 (1978) 147.
7 R. Bonneau and J.M. Kelly, J. Am. Chem. Soc., 102 (1980) 1220.
8 J.A. Welch, K.S. Peters and V. Vaida, J. Phys. Chem., 86 (1982) 1941.
9 J.M. Kelly, D.V. Bent, H. Hermann, D. Shulte-Frohlinde and E.A.K. von Gustorf, J. Organomet. Chem., 69 (1974) 269.
10 J.D. Simon and K.S. Peters, Chem. Phys. Lett., 98 (1983) 53.
11 J.D. Simon and X. Xie, J. Phys. Chem., 90 (1986) 6751.
12 C.H. Langford, C. Moralejo and D.K. Sharma, Inorg. Chim. Acta, 126 (1987) L11.
13 C.H. Langford, A.Y.S. Malkhasian and D.K. Sharma, J. Am. Chem. Soc., 106 (1984) 2727.
14 N. Serpone, D.K. Sharma, J. Moser and M. Gratzel, Chem. Phys. Lett., 136 (1987) 47.
15 L. Persaud, D.K. Sharma and C.H. Langford, Inorg. Chim. Acta, 114 (1986) L5.
16 M. Bernstein, J.D. Simon and K.S. Peters, Chem. Phys. Lett., 100 (1983) 241.

17 R.J. Dennenberg and D.J. Derensbourg, Inorg. Chem., 11 (1972) 72.
18 T.J. Kemp, Prog. React. Kinet., 10 (1980) 301.
19 A.D. Kirk, Coord. Chem. Rev., 39 (1981) 225.
20 A.D. Kirk, P.E. Hoggard, G.B. Porter, M.G. Rockley and M.W. Windsor, Chem. Phys. Lett., 37 (1976) 199.
21 S.C. Pyke and M.W. Windsor, J. Am. Chem. Soc., 100 (1978) 6518.
22 S.C. Pyke, M. Ogasawara, L. Kevan and J.F. Endicott, J. Phys. Chem., 82 (1978) 302.
23 R. Gutierrez and A.W. Adamson, J. Phys. Chem., 82 (1978) 902.
24 R. Ohno and S. Kato, Bull. Chem. Soc. Jpn., 46 (1973) 1602.
25 C.F.C. Wong and A.D. Kirk, Can. J. Chem., 54 (1976) 3794.
26 G. Rojas and D. Magde, Chem. Phys. Lett., 102 (1983) 399.
27 Y.S. Kang, F. Castelli and L.S. Forster, J. Phys. Chem., 83 (1979) 2368.
28 R.T. Walters and A.W. Adamson, Acta Chem. Scand., Ser. A, 83 (1979) 53.
29 R. LeSage, K.L. Sala, R.W. Yip and C.H. Langford, Can. J. Chem., 61 (1983) 2761.
30 B.R. Hollebone, C.H. Langford and N. Serpone, Coord. Chem. Rev., 39 (1981) 181.
31 G. Rojas, C. Dupuy, D.A. Sexton and D. Magde, J. Phys. Chem., 90 (1986) 87.
32 P.C. Ford, Coord. Chem. Rev., 44 (1982) 61.
33 P.C. Ford, D. Wink and T. DiBenedetto, Prog. Inorg. Chem., 30 (1983) 213.
34 C. Creutz, P. Kroger, T. Matsubara, T.L. Netzel and N. Sutin, J. Am. Chem. Soc., 101 (1979) 5442.
35 K.S. Schanze and T.J. Meyer, Inorg. Chem., 24 (1985) 2121.
36 K. Kalyanasundaram, Coord. Chem. Rev., 46 (1982) 159.
37 (a) J.C. Curtis, B.P. Sullivan and T.J. Meyer, Inorg. Chem., 22 (1983) 224.
(b) P.C. Ford, F.P. DeRudd, R. Gaunder and H. Taube, J. Am. Chem. Soc., 90 (1968) 1187.
38 D. Malouf and P.C. Ford, J. Am. Chem. Soc., 99 (1977) 7213.
39 J.R. Winkler, T.L. Netzel, C. Creutz and N. Sutin, J. Am. Chem. Soc., 109 (1987) 2381.
40 (a) N. Sutin and C. Creutz, Adv. Chem. Ser., 168 (1978) 1.
(b) C. Creutz, M. Chou, T.L. Netzel, M. Okumura and N. Sutin, J. Am. Chem. Soc., 102 (1980) 1309.
41 (a) M.A. Bergkamp, J. Brannon, D. Magde, R.J. Watts and P.C. Ford, J. Am. Chem. Soc., 101 (1979) 4549.
(b) M.A. Bergkamp, R.J. Watts and P.C. Ford, J. Am. Chem. Soc., 102 (1980) 2627.
42 M. Talebinasab-Savari, A.W. Zanella and P.C. Ford, Inorg. Chem., 19 (1980) 1835.
43 T.L. Kelly and J.F. Endicott, J. Phys. Chem., 76 (1972) 1937.
44 D.A. Sexton, L.H. Skibsted, D. Magde and P.C. Ford, J. Phys. Chem., 86 (1982) 1758.
45 L.H. Skibsted, D. Strauss and P.C. Ford, Inorg. Chem., 18 (1979) 3171.
46 L.G. Vanquickenborne and A. Ceulemans, J. Am. Chem. Soc., 99 (1977) 2208.
47 D.A. Sexton, P.C. Ford and D. Magde, J. Phys. Chem., 87 (1983) 197.
48 N.J. Linck, S.J. Berens, D. Magde and R.G. Linck, J. Phys. Chem., 87 (1983) 1733.
49 L.H. Skibsted, M.P. Hancock, D. Magde and D.A. Sexton, Inorg. Chem., 23 (1984) 3735.
50 L.H. Skibsted, M.P. Hancock, D. Magde and D.A. Sexton, Inorg. Chem., 26 (1987) 1708.
51 L. Campbell, Ph.D. Thesis, Queen's University of Belfast, Northern Ireland, 1977.
52 G. Lockwood, J.J. McGarvey and R. Devonshire, Chem. Phys. Lett., 86 (1982) 127.
53 L. Vanquickenborne, A. Ceulemans, D. Beyens and J.J. McGarvey, J. Phys. Chem., 86 (1982) 494.
54 (a) C.J. Ballhausen, N. Bjerrum, R. Dingle, K. Eriks and C.R. Hare, Inorg. Chem., 4 (1965) 514.
(b) M. Gerloch, L.R. Hanton and M.R. Manning, Inorg. Chem. Acta, 48 (1981) 205.

55 S.S. Shah and A.W. Maverick, Inorg. Chem., 25 (1986) 1867.
56 C.V. Krishnan, B.S. Brunschwig, C. Creutz and N. Sutin, J. Am. Chem. Soc., 107 (1985) 2005, and references therein.
57 E. Konig and S. Herzog, J. Inorg. Nucl. Chem., 32 (1970) 601.
58 M.S. Henry, J. Am. Chem. Soc., 99 (1977) 6138.
59 M.A. Jamieson and N. Serpone, Coord. Chem. Rev., 39 (1981) 121.
60 N. Serpone and M.Z. Hoffman, J. Chem. Educ., 60 (1983) 853.
61 M.A. Jamieson, N. Serpone and M.Z. Hoffman, J. Am. Chem. Soc., 105 (1983) 2933.
62 N. Serpone, in M. Schiavello (Ed.), Photoelectrochemistry, Photocatalysis and Photoreactors, NATO ASI Series C, Reidel, Dordrecht, 1985, Vol. 146, pp. 351–372.
63 (a) M. Asano, J.A. Koningstein and D. Nicollin, J. Chem. Phys., 73 (1980) 688.
(b) D. Nicollin, P. Bertels and J.A. Koningstein, Can. J. Chem., 58 (1980) 1334.
64 M. Maestri, F. Bolletta, L. Moggi, V. Balzani, M.S. Henry and M.Z. Hoffman, J. Am. Chem. Soc., 100 (1978) 2694.
65 W.H. Woodruff, R.F. Dallinger, M.Z. Hoffman, P.G. Bradley, D. Presser, V. Malueg, R.J. Kessler and K.A. Norton, in G.H. Atkinson (Ed.), Time-resolved spectroscopy, Academic Press, New York, 1983, p. 147.
66 N. Serpone, M.A. Jamieson, D.K. Sharma, R. Danesh, F. Bolletta and M.Z. Hoffman, Chem. Phys. Lett., 104 (1984) 87.
67 F. Castelli and L.S. Forster, J. Phys. Chem., 81 (1977) 403.
68 A.D. Kirk, G.B. Porter and D.K. Sharma, Chem. Phys. Lett., 123 (1986) 548.
69 N. Serpone and M.Z. Hoffman, Chem. Phys. Lett., 123 (1986) 551.
70 G. Rojas and D. Magde, J. Phys. Chem., 91 (1987) 689.
71 N. Serpone and M.Z. Hoffman, J. Phys. Chem., 91 (1987) 1737.
72 A.A. Frost and R.G. Pearson, Kinetics and Mechanisms, Wiley, New York, 1961, pp. 166–171.
73 C. Creutz, M. Chou, T.L. Netzel, M. Okumura and N. Sutin, J. Am. Chem. Soc., 102 (1980) 1309.
74 A.J. Street, D.M. Goodall and R.C. Greenhow, Chem. Phys. Lett., 56 (1978) 326.
75 H.L. Chum, D. Koran and R.A. Osteryoung, J. Am. Chem. Soc., 100 (1978) 310.
76 J. Phillips, J.A. Koningstein, C.H. Langford and R. Sasseville, J. Phys. Chem., 82 (1978) 622.
77 N. Sutin, J. Photochem., 10 (1979) 19.
78 C. Mahon and W.L. Reynolds, Inorg. Chem., 6 (1967) 1927.
79 C.R. Bock, Ph.D. Dissertation, University of North Carolina, Chapel Hill, North Carolina, 1974.
80 M.A. Bergkamp, B.S. Brunschwig, P. Gutlich, T.L. Netzel and N. Sutin, Chem. Phys. Lett., 81 (1981) 147.
81 (a) J.S. Gold, S.J. Milder, J.W. Lewis and D.S. Kliger, J. Am. Chem. Soc., 107 (1985) 8285.
(b) S.J. Milder, J.S. Gold and D.S. Kliger, J. Am. Chem. Soc., 108 (1986) 8295.
82 M.A. Bergkamp, C.-K. Chang and T.L. Netzel, J. Phys. Chem., 87 (1983) 4441.
83 Y.J. Chang, L.K. Orman, D.R. Anderson, T. Yabe and J. Hopkins, J. Chem. Phys., 87 (1987) 3249.
84 P.G. Bradley, N. Kress, B.A. Hornberger, R.F. Dallinger and W.H. Woodruff, J. Am. Chem. Soc., 103 (1981) 7441.
85 M. Forster and R.E. Hester, Chem. Phys. Lett., 81 (1981) 42.
86 J.V. Caspar, T.D. Westmoreland, G.H. Allen, P.G. Bradley, T.J. Meyer and W.H. Woodruff, J. Am. Chem. Soc., 106 (1984) 3492.

87 L.A. Philips, W.T. Brown, S.P. Webb, S.W. Yeh and J.H. Clark, in D.H. Auston and K.B. Eisenthal (Eds.), Proc. 4th Int. Conf. on Ultrafast Phenomena, Springer, Berlin, 1984, p. 390.
88 N. Kitamura, H.B. Kim, Y. Kaawanishi, R. Obata and S. Tazuke, J. Phys. Chem., 90 (1986) 1488.
89 E. Krausz, Chem. Phys. Lett., 116 (1986) 501.
90 J. Ferguson, E.R. Krausz and M. Mader, J. Phys. Chem., 89 (1985) 1852.
91 M.A. Bergkamp, P. Gutlich, T.L. Netzel and N. Sutin, J. Phys. Chem., 87 (1983) 3877.
92 T. Kobayashi and Y. Ohashi, in R. Hochstrasser, W. Kaiser and C.V. Shank (Eds.), Picosecond Phenomena, Springer, Berlin, 1980, Vol. 2, p. 181.
93 T. Kobayashi and Y. Ohashi, Chem. Phys. Lett., 86 (1982) 289.
94 Y. Ohashi and T. Kobayashi, Bull. Chem. Soc. Jpn., 52 (1979) 2214.
95 Y. Ohashi and T. Kobayashi, J. Phys. Chem., 83 (1979) 551.
96 P. Day and N. Sanders, J. Chem. Soc. A, (1967) 1536.
97 C.C. Phifer and D.R. McMillin, Inorg. Chem., 25 (1986) 1329.
98 D.R. McMillin, R.E. Gamache, Jr., J.R. Kirchhoff and A.A. DelPaggio, in K.D. Karlin and J. Zubieta (Eds.), Copper Coordination Chemistry: Biochemical and Inorganic Perspectives, Adenine, New York, 1986, pp. 223–235.
99 M.W. Blaskie and D.R. McMillin, Inorg. Chem., 19 (1980) 3519.
100 E.L. Wehry and S. Sundarajan, J. Chem. Soc., Chem. Commun., (1972) 1135.
101 G. Blasse, P.A. Breddels and D.R. McMillin, Chem. Phys. Lett., 109 (1984) 24.
102 D.R. McMillin, J.R. Kirchhoff and D.V. Goodwin, Cood. Chem. Rev., 64 (1985) 83.
103 P.J. Burke, K. Henrick and D.R. McMillin, Inorg. Chem., 12 (1982) 1881.
104 M. Van Meerssche, G. Germain, J.P. Declercq and L. Wilputte-Steinert, Cryst. Struct. Commun., 10 (1981) 47.
105 C.E.A. Palmer, D.R. McMillin, C. Kirmaier and D. Holten, Inorg. Chem., 26 (1987) 3167.
106 C.D. Cowman and H.B. Gray, J. Am. Chem. Soc., 95 (1973) 8177.
107 F.A. Cotton, D.S. Martin, P.E. Fanwick, T.J. Peters and T.R. Webb, J. Am. Chem. Soc., 98 (1976) 4681.
108 P.E. Fanwick, D.S. Martin, F.A. Cotton and T.R. Webb, Inorg. Chem., 16 (1977) 2103.
109 C.D. Cowman, W.C. Trogler and H.B. Gray, Isr. J. Chem., 15 (1977) 308.
110 W.C. Trogler, C.D. Cowman, H.B. Gray and F.A. Cotton, J. Am. Chem. Soc., 99 (1977) 2993.
111 W.C. Trogler and H.B. Gray, Acc. Chem. Res., 11 (1978) 232.
112 V.M. Miskowski, R.A. Goldbeck, D.S. Kliger and H.B. Gray, Inorg. Chem., 18 (1979) 86.
113 S.F. Rice, R.B. Wilson and E.I. Solomon, Inorg. Chem., 19 (1980) 3425.
114 P.J. Hay, J. Am. Chem. Soc., 104 (1982) 7007.
115 M.D. Hopkins, T.C. Zietlow, V.M. Miskowski and H.B. Gray, J. Am. Chem. Soc., 107 (1985) 510.
116 K.B. Mathisen, U. Wahlgren and L.G.M. Pettersson, Chem. Phys. Lett., 104 (1984) 336.
117 U. Stromberg, Chem. Phys. Lett., 118 (1985) 389.
118 I.F. Fraser and R.D. Peacock, Chem. Phys. Lett., 98 (1983) 620.
119 M.D. Hopkins and H.B. Gray, J. Am. Chem. Soc., 106 (1984) 2468.
120 T.C. Zietlow, M.D. Hopkins and H.B. Gray, J. Solid State Chem., 57 (1985) 112.
121 J.R. Winkler, D.G. Nocera and T.L. Netzel, J. Am. Chem. Soc., 108 (1986) 4451.
122 R.H. Flemming, G.L. Geoffroy, H.B. Gray, A. Gupta, G.S. Hammond, D.S. Kliger and V.M. Miskowski, J. Am. Chem. Soc., 98 (1976) 48.

123 S.F. Rice and H.B. Gray, J. Am. Chem. Soc., 103 (1981) 1593.
124 R.F. Dallinger, V.M. Miskowski, H.B. Gray and W.H. Woodruff, J. Am. Chem. Soc., 103 (1981) 1595.
125 S.F. Rice and H.B. Gray, J. Am. Chem. Soc., 105 (1983) 4571.
126 J.L. Marshall, S.R. Stobart and H.B. Gray, J. Am. Chem. Soc., 106 (1984) 3027.
127 C.-M. Che, S.J. Atherton, L.G. Butler and H.B. Gray, J. Am. Chem. Soc., 106 (1984) 5143.
128 J.R. Winkler, J.L. Marshall, T.L. Netzel and H.B. Gray, J. Am. Chem. Soc., 108 (1986) 2263.
129 K.R. Mann, J.A. Thich, R.A. Bell, C.L. Coyle and H.B. Gray, Inorg. Chem., 19 (1980) 2462.
130 J.V. Caspar and H.B. Gray, J. Am. Chem. Soc., 106 (1984) 3029.
131 L.S. Fox, J.L. Marshall, H.B. Gray and J.R. Winkler, J. Am. Chem. Soc., 109 (1987) 6901.
132 B.T. Reagor, D.F. Kelley, D.H. Huchital and P.M. Rentzepis, J. Am. Chem. Soc., 104 (1982) 7400.
133 L. Rosenheim, D. Spencer and A. Haim, Inorg. Chem., 13 (1974) 1571.
134 D.H. Huchital and J. Lepore, Inorg. Chem., 17 (1978) 1134.
135 B.T. Reagor, Ph.D. Dissertation, Seton Hall University, South Orange, NJ, 1982, Section III-A,B; quoted in ref. 132.
136 D.H. Huchital and R.G. Wilkins, Inorg. Chem., 6 (1967) 1022.
137 A. Vogler and J. Kisslinger, Angew. Chem., 21 (1982) 77.
138 C. Creutz, P. Kroger, T. Matsubara, T.L. Netzel and N. Sutin, J. Am. Chem. Soc., 101 (1979) 5442.
139 H. Fisher, G.M. Tom and H. Taube, J. Am. Chem. Soc., 98 (1976) 5512.
140 J.P. Collman, Acc. Chem. Res., 10 (1977) 265, and references therein.
141 E.F. Hilinski and P.M. Rentzepis, Nature, 302 (1983) 481, and references therein.
142 K.M. Smith (Ed.), Porphyrins and Metalloporphyrins, Elsevier, New York, 1975.
143 F. Basolo, B.M. Hoffman and J.A. Ibers, Acc. Chem. Res., 8 (1975) 384.
144 J.T. Spence, Coord. Chem. Rev., 4 (1968) 475.
145 Y. Matsuda, S. Yamada and Y. Murakami, Inorg. Chem., 20 (1981) 2239.
146 M. Gouterman, in D. Dolphin (Ed.), The Porphyrins, Academic Press, New York, 1978, Vol. III, Part A, Chap. 1, p. 1.
147 K. Kalyanasundaram and M. Graetzel, Helv. Chim. Acta, 63 (1980) 478.
148 A. Harriman and M.C. Richoux, J. Photochem., 14 (1980) 253.
149 A. Harriman, G. Porter and M.C. Richoux, J. Chem. Soc. Faraday Trans. 2, (1975) 1175.
150 A. Harriman, G. Porter and M.C. Richoux, J. Chem. Soc. Faraday Trans. 2, (1981) 833.
151 T.L. Netzel, P. Kroger, C.-K. Chang, I. Fujita and J. Fajer, Chem. Phys. Lett., 67 (1979) 223.
152 I. Fujita, J. Fajer, C.-K. Chang, C.-B. Wang, M.A. Bergkamp and T.L. Netzel, J. Phys. Chem., 86 (1982) 3754.
153 N. Serpone, H. Ledon and T.L. Netzel, Inorg. Chem., 23 (1984) 454.
154 Y. Matsuda, F. Kubota and Y. Murakami, Chem. Lett., (1977) 1281.
155 (a) H.J. Ledon and B. Mentzen, Inorg. Chim. Acta, 31 (1978) L393.
(b) T.S. Srivastava and E.B. Fleischer, J. Am. Chem. Soc., 92 (1970) 5518.
156 H.J. Ledon, M.C. Bonnet, Y. Brigandat and F. Varescon, Inorg. Chem., 19 (1980) 3488.
157 J.W. Buchler, W. Kokisch and P.D. Smith, Struct. Bonding (Berlin), 34 (1978) 79.
158 D. Magde, M.W. Windsor, D. Holton and M. Gouterman, Chem. Phys. Lett., 29 (1974) 183.

159 A. Antipas, J.W. Buchler, M. Gouterman and P.D. Smith, J. Am. Chem. Soc., 100 (1978) 3015; 102 (1980) 198.
160 N. Serpone, T.L. Netzel and M. Gouterman, J. Am. Chem. Soc., 104 (1982) 246.
161 G. Ponterini, N. Serpone, M.A. Bergkamp and T.L. Netzel, J. Am. Chem. Soc., 105 (1983) 4639.
162 T. Kobayashi, K.D. Straub and P.M. Rentzepis, Photochem. Photobiol., 29 (1979) 925.
163 J.B. Callis, M. Gouterman, Y.M. Jones and R.H. Henderson, J. Mol. Spectrosc., 39 (1971) 410.
164 T.L. Netzel and I. Fujita, unpublished observations, quoted in ref. 151.
165 (a) D.J. Quimby and F.R. Longo, J. Am. Chem. Soc., 97 (1975) 5111.
(b) P.G. Seybold and M. Gouterman, J. Mol. Spectrosc., 31 (1969) 1.
166 (a) G.P. Gurinovich and B.M. Dzhagarov, Izv. Akad. Nauk SSSR, Ser. Fis., 37 (1973) 383.
(b) G.P. Gurinovich, A.I. Patsko and A.N. Sevchenko, Dokl. Akad. Nauk SSSR, 174 (1967) 873.
167 G. Maki, J. Chem. Phys., 29 (1958) 651, 662 and 1129.
168 R.L. Ake and M. Gouterman, Theor. Chim. Acta, 17 (1970) 408.
169 A. Adamczyk and F. Wilkinson, J. Chem. Soc., Faraday Trans. 2, 68 (1972) 2031.
170 M.P. Tsvirko, K.N. Solovev and V.V. Sapinov, Opt. Spectrosc., 36 (1975) 193.
171 R.L. Ake and M. Gouterman, Theor. Chim. Acta, 15 (1969) 20.
172 T. Kobayashi, D. Huppert, K.D. Straub and P.M. Rentzepis, J. Chem. Phys., 70 (1979) 1720.
173 A. Antipas, D. Dolphin, M. Gouterman and E.C. Johnson, J. Am. Chem. Soc., 100 (1978) 7705.